



**US Army Corps
of Engineers®**
Engineer Research and
Development Center

Extending the Season for Concrete Construction and Repair

Phase II—Defining Engineering Parameters

Charles J. Korhonen

April 2006

Extending the Season for Concrete Construction and Repair

Phase II—Defining Engineering Parameters

Charles J. Korhonen

*Cold Regions Research and Engineering Laboratory
U.S. Army Engineer Research and Development Center
72 Lyme Road
Hanover, NH 03766*

Final report

Approved for public release; distribution is unlimited.

Prepared for U.S. Federal Highway Administration

Under Program Project TPF-5(075)

Abstract: The Phase I study, conducted prior to the work reported herein, developed the tools to design, mix, place, and cure concrete in cold weather made with various combinations of commercial admixtures. The admixtures helped to protect concrete and maintain productivity, even when the temperature of concrete falls to -5°C soon after mixing. Phase II addressed the effect of high doses of the chemical admixtures studied in Phase I. The primary finding from Phase I that led to this study was that admixtures, when used in moderate dosages, seemed to improve the freeze–thaw durability of concrete. Phase II found what appears to be a maximum dosage after which freeze–thaw durability becomes a concern. That is because cement hydration can only create a finite amount of space to absorb these chemicals. Thus, for freeze protection, admixture dosages should be designed according to water content as specified in Phase I, while, for freeze–thaw durability, admixture dosages should be dictated by cement content. When using both considerations, the freeze-protection limit for enhanced freeze–thaw durable concrete can be lower than the -5°C limit set in Phase I.

DISCLAIMER: The contents of this report are not to be used for advertising, publication, or promotional purposes. Citation of trade names does not constitute an official endorsement or approval of the use of such commercial products. All product names and trademarks cited are the property of their respective owners. The findings of this report are not to be construed as an official Department of the Army position unless so designated by other authorized documents.

DESTROY THIS REPORT WHEN NO LONGER NEEDED. DO NOT RETURN IT TO THE ORIGINATOR.

Contents

Figures and Tables	v
Preface	vii
1 INTRODUCTION	1
2 LITERATURE REVIEW	2
3 EXPERIMENTAL PROCEDURE.....	6
Materials	6
Cement	6
Fine aggregate	6
Water	7
Admixtures.....	7
Control mortar	8
Antifreeze mortar	9
Mixing procedures.....	9
Sample preparation and curing	10
Testing Procedures.....	11
Freezing point.....	11
Strength.....	12
Fundamental frequency.....	14
Length change.....	15
4 RESULTS AND DISCUSSION	18
Freezing point	18
Freeze-thaw resistance.....	22
Control mortar	23
Antifreeze mortar	25
Length change of mortar bars.....	28
Control Mortar	29
Antifreeze Mortar	33
Salt scale	34
5 SUMMARY AND CONCLUSIONS	37
6 NEEDED RESEARCH.....	39
7 REFERENCES.....	40
APPENDIX A: Batch proportions	43
APPENDIX B: Freeze-thaw data from individual mortar beams	48

**APPENDIX C: Relationship between length-change and temperature for antifreeze
mortar beams60**

Report Documentation Page.....75

Figures and Tables

Figures

Figure 1. Length change after 300 freezing and thawing cycles as a function of the average distance between air bubbles.....	2
Figure 2. Surface scaling vs. solution concentration for four chemicals.....	3
Figure 3. Durability of concrete with admixture concentrations given as percent by cement weight.....	5
Figure 4. Typical cooling curves taken from freezing-point measurements.....	11
Figure 5. Typical freezing and thawing cycles.....	14
Figure 6. Dilation box.	15
Figure 7. Results of cooling and warming an aluminum beam in the length-change test device.....	17
Figure 8. Freezing point versus concentration of solid admixture by weight of water based on Table 6 data plus a few extra confirmatory tests not shown in Table 6.....	19
Figure 9. Effect of admixture dosage on the 28-day compressive strength of mix 5 mortar	20
Figure 10. Compressive strength versus air content.	22
Figure 11. Performance of non-air-entrained mortar subjected to cycles of freezing and thawing..	24
Figure 12. Effect of air content on freeze-thaw durability of four control beams from Mix 5.	26
Figure 13. Time-temperature cooling curve used to determine the freezing point (-17°C) of hardened mortar (Mix 8) made with admixture MBIV at 16% concentration by weight of water.....	27
Figure 14. Length-change curves for non-air-entrained control mortar beams subjected to cooling cycle.....	30
Figure 15. Effect of using saltwater to surround beams during freeze-thaw testing control and antifreeze concrete made from mix 5.....	36
Figure 16. Visual survey of bridge repair after exposure to two New England winters.....	36

Tables

Table 1. Comparison of the Type I/II cement used in this study to that typical of Type I and II portland cements.....	6
Table 2. Fine aggregate sieve analysis.	7
Table 3. Admixtures along with their dosage ranges compared to the maximum dosage recommended by the manufacturer.	7
Table 4. Mortars developed from each of five concrete mix designs.	8
Table 5. Admixture application rates for the series of antifreeze mortars based on control mix 5.	9
Table 6. Freezing points measured at initiation of freezing.....	18
Table 7. Temperature, estimated to the nearest degree Celsius, that mortar beams first began to expand.	34
Table 8. The number of freeze–thaw cycles before specimens made from Mix 5 reached 60% RDME.	35

Preface

This report was prepared by Charles J. Korhonen, Research Civil Engineer, Civil Engineering and Infrastructure Branch, U.S. Army Engineer Research and Development Center (ERDC), Cold Regions Research and Engineering Laboratory (CRREL), Hanover, New Hampshire. The work was funded by the FHWA pooled-fund program project TPF-5(075). The author wishes to acknowledge the nine state departments of transportation that used SP&R funds to support this work: Idaho, Michigan, Montana, New Hampshire, New York, Pennsylvania, Vermont, Wisconsin, and Wyoming. In addition, the following are acknowledged for their contributions to this project: Jack Bayer, Civil Engineering Technician, CRREL, for his assistance in fabricating test samples, curing them, and evaluating them under laboratory conditions; and Bill Piper, Lead Custodian, CRREL, for carefully and faithfully monitoring the freeze–thaw cabinets, making sure that they continued to function day-to-day, and for reporting malfunctions when they arose.

Roger Apple (PA) and Craig Graham (VT) technically reviewed this report.

This report was prepared under the general supervision of James Buska, Acting Chief, Geophysical Sciences Branch; Lance Hansen, Acting Deputy Director; and James Wuebben, Acting Director, CRREL. The Commander and Executive Director of the Engineer Research and Development Center is COL James R. Rowen. The Director is Dr. James R. Houston.

1 INTRODUCTION

Phase I, *Establishing the Technology*, of Federal Highway Administration pooled-fund study TPF-5(003), *Extending the Season for Concrete Construction and Repair*, established the practicality of mixing, transporting, placing, and finishing concrete made with commercially available admixtures as antifreeze admixtures. Concrete made with combinations of off-the-shelf additives fully cured while its internal temperature was -5°C and was at least as durable as normal concrete. Other benefits noted during the study included both time- and cost-saving advantages. Specifically, the concrete construction season can be extended by 60 to 120 days in cold regions and, because less thermal protection is required, the emplaced cost could be one-third less compared to conventional cold-weather concreting techniques (Korhonen et al. 2004). Following this study, ASTM (2005) C 1622, *Standard Specification for Cold-Weather Admixture Systems*, was published (Korhonen and Jeknavorian 2005), formally qualifying antifreeze admixtures and providing assurance that they are effective.

An unexpected result from the Phase I freeze–thaw testing led to the work reported herein. Though antifreeze admixtures were found not to reduce the freeze–thaw durability of concrete, surprisingly, they seemed at times to improve it. This intriguing finding triggered a more in-depth look at the effect that antifreeze admixtures have on durability: the literature was consulted and tests were repeated. Again, testing showed that some antifreeze concretes turned out to be more freeze–thaw durable than control concrete, and the literature showed that chemical additives have been documented to enhance concrete’s durability under certain conditions. The potentially huge benefit that admixtures might have on highway maintenance budgets by creating more durable concrete could not be overlooked. Thus, this work studied the possible beneficial effect of chemical admixtures on the freeze–thaw durability of concrete.

2 LITERATURE REVIEW

The number one problem of concrete in cold climates is deterioration caused by freezing and thawing. Several theories have been developed to explain frost damage, but it is well known that such damage only happens to moist concrete. The movement of water, either toward or away from the freezing front, amplifies this damage, as does a high degree of saturation coupled with rapid cooling. Air entrainment is today's defense against frost damage (Fig. 1). It provides empty reservoirs within the cement paste into which pressurized water and ice can escape. Little attention has been devoted to possible beneficial effects that altering the pore water chemistry might have on the freeze–thaw durability of concrete. Though chemicals are routinely used in just about all modern concrete mixtures, there is no evidence that they negatively affect concrete's durability when used as recommended.

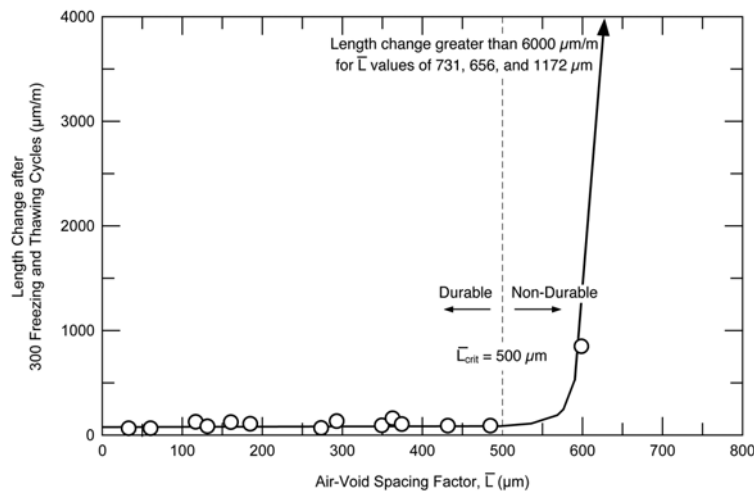


Figure 1. Length change after 300 freezing and thawing cycles as a function of the average distance between air bubbles. (After Pigeon et al. 1986.)

Part of the reticence of considering chemicals to improve durability is ascribable to the widespread pavement scaling that has been attributed to deicing salts. It was during the 1920s and 1930s that high-speed highways, usable under all weather conditions, created the need for deicing salts (Whiting and Stark 1983). By the mid-1930s, however, many concrete pavements in the northern states had seriously scaled, presumably because of the deicing salts. The scaling, which usually developed within 2

years after salt was first used, was eventually related to the amount of salt applied to the road and to the frequency of application. Numerous experiments conducted since then describe the role that salt plays in the destruction of concrete pavement.

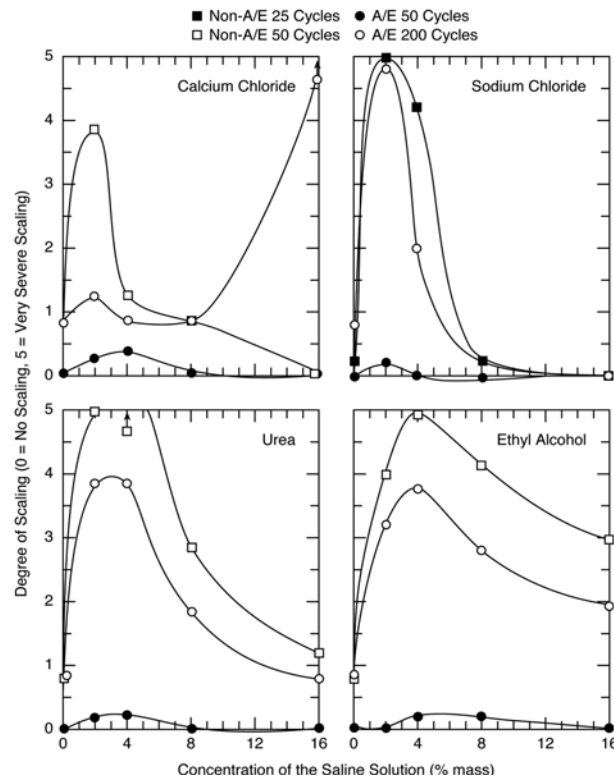


Figure 2. Surface scaling vs. solution concentration for four chemicals. A/E stands for air-entrained. (After Verbeck and Klieger 1957.)

An early influential study in North America about salt action in concrete is that done by Verbeck and Klieger (1957). They applied chemical solutions of various concentrations on the upper surface of concrete slabs, which were saturated with plain water, before, during, and after freezing and observed their effects as a function of freeze–thaw cycle. One finding was that freezing and thawing a specimen with a salt solution on the surface was more severe than applying such a solution to an already frozen specimen. The least severe response came from specimens that were frozen in a damp condition, after having removed the salt solution from the surface. Aside from proving that salt exacerbates surface scaling, the more interesting finding was that a solute concentration of 3–4% produced more surface scaling than did higher or lower concentrations, including pure water. Verbeck and Klieger studied four chemicals, finding that all were similar in action, which seemingly demonstrated that surface scaling was a physical

and not a chemical process (Fig. 2). Higher concentrations progressively produced lesser scaling to where at approximately 13% the damage was equal to that for plain water, and that at higher concentrations, scaling became even less pronounced than that for plain water.

Other studies since then have found similar results. Litvan (1976), by measuring length change of paste specimens as they cooled in a saturated condition inside a sealed testing cell, found that, when impregnated with NaCl solutions at various concentrations, the length change curves were similar to those of specimens containing no salt, but they differed in magnitude. Litvan showed that 5% salt solutions produce dilation five times larger than that of plain water.

Fagerlund (1997) reported that mortar saturated with 5 and 10% NaCl solutions expanded less than did plain mortar. The largest expansion in his experiments occurred when the water in the pores of the mortar contained 2.5% salt solution.

Sellevoid and Farstad (1991) found that when salt solutions are applied to the outer surface of concrete, scaling is more pronounced for specimens that are water-saturated compared to those saturated with a salt solution prior to testing. They also demonstrated through calorimetry that the freezing point of bulk water in the pores of cement paste is depressed by the presence of dissolved ions in the water.

Where antifreeze admixtures have been studied, scaling was not noted as a problem. Kukko and Koskinen (1988) describe admixtures, 20% and above by weight of mixing water, that when added to fresh concrete did not create a problem with scaling in freeze–thaw tests. In fact, Grapp et al. (1975) report that the freeze–thaw durability of concrete beams made with certain antifreeze chemicals was superior to normal concrete (Fig. 3). Potash ash (K_2CO_3) was one chemical found to reduce concrete's freeze–thaw resistance, whereas the other chemicals tested showed (Fig. 3) a marked improvement in freeze–thaw durability compared to control concrete. Interestingly, several beams even became more durable to frost damage during the course of testing.

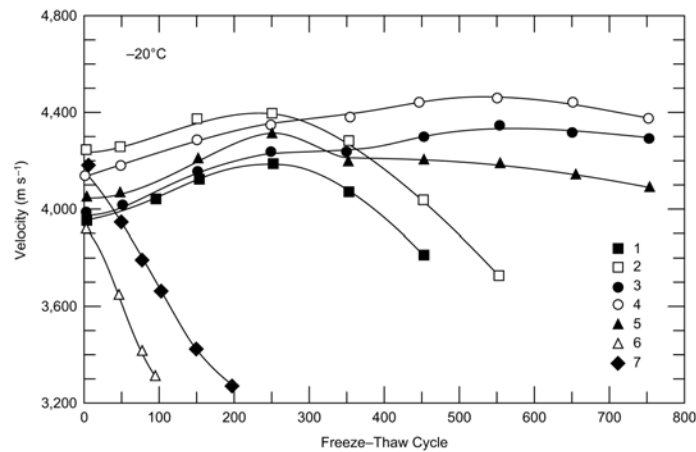


Figure 3. Durability of concrete with admixture concentrations given as percent by cement weight (w/c ratio 3:1) (after Grapp et al. 1975). 1—Control without air-entraining admixture; 2—15% NaNO₂; 3—15% Ca(NO₃)₂; 4—15% Ca(NO₃)₂ / (NO₂)₂ + CaCl₂ + CO(NH₂)₂; 5—15% CaCl₂ + NaNO₂; 6—15% K₂CO₃; 7—25% K₂CO₃.

In summary, the literature survey of laboratory test results pointed out that a salt solution can either accelerate or retard scaling damage, depending on the concentration of the solution to which the concrete is subjected. It also revealed that when chemicals are intentionally added into fresh concrete, both scaling resistance and freeze-thaw durability can sometimes be improved. It was clear that work was needed to understand how the chemicals studied in Phase I affect the freeze-thaw performance of concrete so that better use may be made of them.

3 EXPERIMENTAL PROCEDURE

Materials

All materials, i.e., cement, aggregate, water, and chemicals, were commercially available and met applicable standards for concrete-making materials. No attempt was made to enhance the performance of test specimens by use of materials unapproved for use in concrete.

Cement

The cement came from the same source used in the laboratory studies of Phase I. Unlike Phase I, where many different lots of cement were used over a 3-year period, this study used one lot. It was carefully protected from moisture throughout the duration of laboratory testing. The cement was an ASTM (2002b) C 150 Type I/II portland cement from Lafarge North America. Table 1 shows the chemical and physical composition of the cement compared to that typical of Type I and Type II cements in the U.S.

Table 1. Comparison of the Type I/II cement used in this study to that typical of Type I and II portland cements.

Compound	Type I*	Type II*	Type I/II
Tricalcium silicate	50	45	54
Dicalcium silicate	25	30	18
Tricalcium aluminate	12	7	8
Tetracalcium alumino-ferrite	8	12	9
Fineness (Blaine, m ² /kg)	350	350	370

* Data from Mindess and Young (1981).

Fine aggregate

The fine aggregate was an ASTM (1997a) C 33 natural siliceous sand having bulk specific gravity of 2.72 (saturated surface dry), absorption of 0.9%, dry rodded unit weight of 1736 kg/m³, and fineness modulus of 2.78. A sieve analysis for the fine aggregate compared to ASTM requirements is given in Table 2.

Table 2. Fine aggregate sieve analysis.

Sieve	Percent Passing	ASTM C33
4.75 mm	100.0	95-100
2.36 mm	89.0	80-100
1.18 mm	66.3	50-85
600 μm	41.5	25-60
300 μm	8.6	10-30
150 μm	6.5	2-10
75 μm	3.3	0-5

Water

The water used in this study was potable water from the town of Hanover, New Hampshire. Its pH was approximately 6.3 and it was used directly from the tap at temperatures between 7 and 10°C.

Admixtures

The MB-IV admixtures used in Phase I were chosen for this study, except that Glenium 3000 NS was used in place of Polyheed 997 (Table 3). Chemically, this admixture combination represents the other seven admixture combinations described in the Phase I study (Korhonen et al., 2004): they contained calcium nitrite-based corrosion inhibitors and accelerators in addition to water reducers. Table 3 shows the dosage range used for each additive to achieve the various admixture concentrations used in this study. As can be seen, the corrosion inhibitor and accelerator exceeded the maximum allowable limit set by the manufacturer for general concrete mixes. Usage rates outside the recommended dosage range were intentionally used to explore the effect of very high dosages on durability.

Table 3. Admixtures along with their dosage ranges compared to the maximum dosage recommended by the manufacturer.*

Admixture	Function	Dosage Range	Recommended Maximum Dosage
Rheocrete CNI (L/m ³)	Corrosion Inhibitor	2.0-63.6	30
Pozzutec 20+ (L/100 kg)	Accelerator	0.39-12.6	5.87
Glenium 3000 NS (mL/100 kg)	Plasticizer	0-243	780

* Degussa

Mortar vs. concrete

Instead of concrete, non-air-entrained mortar was used to evaluate the performance of the admixtures, except when entrained air voids were be-

ing evaluated. Non-air-entrained mortar was used to avoid confounding the results with entrained air voids that can differ from sample to sample. No attempt was made to remove or otherwise modify entrapped air voids. Using mortar simplified mixing operations, reduced materials handling, and permitted smaller test specimens. To the admixtures, mortar behaves like concrete; it uses cement and water, it has void spaces, and it has aggregate-to-paste transition zones. The main difference between mortar and concrete is that mortar does not contain coarse aggregate.

Control mortar

Five control mortars, each patterned after a concrete mixture with a different w/c ratio, were used to assess the effect of admixture dosage, cement content, and w/c (water/cement) ratio on freezing point depression, strength development, and freeze–thaw durability. Each mortar was designed to match the mortar fraction of existing concrete mixtures by estimating the quantity of cement paste needed to fill the interstitial voids in the sand fraction of a concrete mixture, subtracting it from the total paste volume in the concrete, and then using the resulting volume to calculate the thickness of paste needed to uniformly coat the sand and coarse aggregate in that concrete. Hence, the mortar design consisted of sand, the paste needed to fill interstitial voids, and paste needed to coat the sand particles. Table 4 presents the mixture proportions used for each mortar compared to its concrete counterpart.

Table 4. Mortars developed from each of five concrete mix designs. The sand/cement ratio considers sand to be saturated surface dry.

Mix number*	Type	Cement (kg/m ³)	W/C	Sand/cement**
5	Concrete	362	0.47	2.31
	Mortar	—		2.35
6	Concrete	390	0.44	2.05
	Mortar	—		2.09
8	Concrete	474	0.36	1.55
	Mortar	—		1.59
9	Concrete	502	0.34	1.43
	Mortar	—		1.47
11	Concrete	558	0.30	1.21
	Mortar	—		1.25

* Eleven mixes were initially developed for this study, from which these five were selected.

** For comparison, ASTM (1989) C 109 uses a 2.75 ratio.

Antifreeze mortar

A series of antifreeze mortars were made from each of the controls to test the effect of admixture concentration on their performance. For example, Table 5 shows the series of mortars developed from control 5. (Appendix A provides the laboratory mix sheets for all mortars used in this study.) As can be seen, the antifreeze mortars contained admixture concentrations from 0 to 24%, based on the solids content of the additives to the weight of water in the mix. The sand to cement and water to cement ratios shown in Table 4 remained constant for all mortars in this study.

Table 5. Admixture application rates for the series of antifreeze mortars based on control mix 5.

Mix #/ Concentration*	Rheocrete CNI (L/m ³)	Pozzutec 20+ (L/100 kg)	Glenium 3000 NS** (mL/100 kg)
5/0	0	0	0
5/1	2.72	0.52	0
5/3	7.92	1.56	0
5/6	15.84	3.13	0
5/9	23.76	4.76	0
5/12	31.69	6.32	0
5/16	42.08	8.41	0
5/20	52.98	10.50	0
5/24	63.62	12.58	0

* Concentration represents the weight of solids added to the mortar by the admixtures divided by the weight of free water in the mortar in percent.

** Glenium was used only as needed to maintain workability from mix to mix. It was not needed in this mix. When used at its largest dosage, mix 11 at 360 mL/100 kg, the freezing point of the mix was essentially unchanged.

Mixing procedures

All mortars were mixed in a 10-L capacity Hobart mixer according to ASTM C 305 (1987) at room temperature. The batch size of each mixture was approximately 7.2 L. The sand and cement were stored at room temperature between 23 and 27°C, while the water was obtained directly from the taps at a temperature between 7 and 10°C. Moisture contents for the sand were determined prior to mixing by drying approximately a 200-g sample in a microwave oven and then adjusting the mixture water accordingly.

The corrosion inhibitor, accelerator, and mixing water were the first ingredients to be placed into the mixing bowl. The mixer was then run at low

speed for 30 seconds while the cement was added in to the bowl. Mixing was stopped, the sides of the bowl were scraped down, and the mixer was run for another 45 seconds while sand was added. The mixer was stopped for a minute and a half before the high-range water reducer, if needed, was added with the mixer running at medium speed for the final minute. The water reducer was added during the first 15 seconds of the final mixing period. (Several trials were conducted to determine the optimum time to add the water reducer to the mix. Neither adding the water reducer immediately with the total mixing water nor delaying addition with one-third of the mixing water after the initial 30-second mixing period was as effective at increasing the mobility of the mix as was adding the admixture after all the aggregate, cement, and total water were partially mixed.) The entire mixing procedure lasted 4 minutes. Test samples were immediately placed into molds following mixing.

Sample preparation and curing

Three different molds were used, depending upon the testing requirements. Strength and freezing point samples were cast into 50.8- × 101.6-mm plastic cylindrical molds, freeze–thaw specimens were cast in steel prism molds measuring 76.2 × 76.2 × 304.8 mm, and length-change specimens were cast in reusable plastic molds measuring 12.7 × 25.4 × 254 mm. All samples were vibrated on a table to ensure consolidation and struck off with a magnesium float. The molds were then capped with plastic lids or covered with cellophane, as appropriate, and stored in a 20°C room maintained at approximately 90% RH, except for the freezing point samples, which were immediately placed into a –20°C room. All samples were placed into the temperature-controlled rooms within 30 minutes after water first contacted cement. The strength specimens remained sealed and in their respective rooms until the time for testing. All other specimens were stripped of their molds within 24 hours following casting, identified with a permanent marker, placed in room temperature, lime-saturated water for 27 days, and then stored at 50% RH and 23±3°C until testing. Prior to testing, all specimens were placed in lime-saturated water for 24 hours.

Testing Procedures

Freezing point

Freezing points were measured by embedding thermocouples into 50.8- × 101.6-mm cylinders of fresh mortar placed into a -20°C room. Figure 4 shows a typical cooling curve for an antifreeze mortar compared to that of tap water and control mortar. The freezing point on each curve is identified as the approximate location where the slope of the cooling curves changed. Note that at that location, both mortars slightly supercooled before suddenly warming up a matter of tenths of a degree. The lowest supercooling represents the temperature at which ice spontaneously nucleates, releasing the latent heat that warms the system, while the highest rebound temperature defines where ice grows (i.e., the freezing point).

As can be seen, water solidifies at one temperature—remaining at approximately -0.04°C throughout freezing. While heat was continually removed from the water, the heat of fusion released by the phase change kept the temperature constant until nearly all of the water froze. At that point the temperature of the ice dropped until it equilibrated with its surroundings.

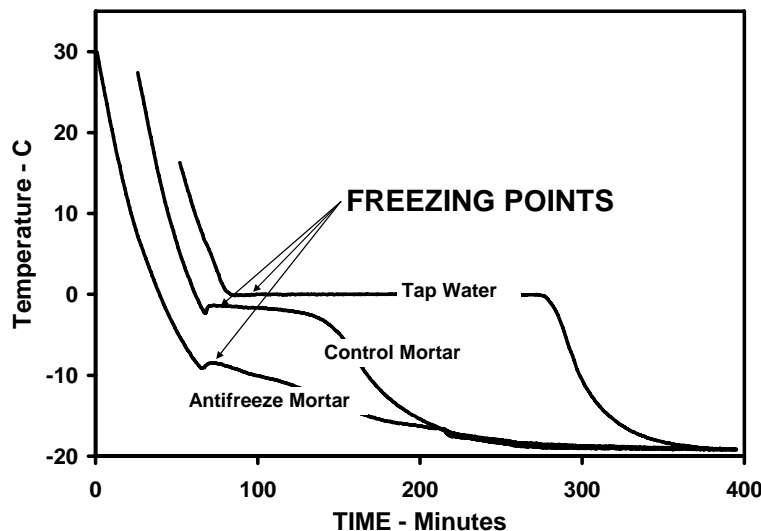


Figure 4. Typical cooling curves taken from freezing-point measurements.

Conversely, the mortars with a solution, as opposed to pure liquid, did not have a single point freezing temperature. As these solutions froze, the solid formed was pure ice. And, as the ice separated out from solution, the concentration of solutes in the remaining solution correspondingly increased,

requiring progressively lower temperatures to grow more ice. As can be seen, the control mortar initially froze at -1.3°C and only needed to drop a half degree more before the entire solution solidified. (Typically, control mortars in other tests at CRREL have had initial freezing points between -0.5 and -1.5°C , regardless of the w/c ratio used to make the mortar.)

The antifreeze mortar first produced ice at -8.5°C but it probably never completely froze as it did not display the rapid drop off in temperature seen for the control once all liquid water froze. A colder room would be needed to determine if such a drop would actually occur. Interestingly, Mironov (1977) showed that if the quantity of ice produced during a freezing event could be controlled, as Figure 4 suggests that it can be if the temperature does not drop too low, the concrete will not be harmed. He suggested that 20% of the mix water can freeze without harming the ultimate strength of the concrete. This has interesting implications for winter concreting in the U.S., where outdoor temperatures are not too severe. The effect of ice content on the resulting quality of concrete were not pursued. In this study, -8.5°C would be considered the freezing point of the mortar, even though only some of the water turned to ice at that temperature.

Strength

The Phase I study documented the strength development of antifreeze mortar at low temperatures. This study investigated the effect of admixture dosage on the ultimate strength of mortar at room temperature. Knowing that there is a finite volume within mortar into which the admixtures can reside, we felt that, at high enough dosages, the strength of mortar might be reduced, and this could, in turn, compromise freeze–thaw durability. Three samples of each mortar made with a different dosage of admixture were tested in uniaxial compression according to ASTM (1997b) C 39 at 28 days. Each sample was capped with unbonded neoprene held within a steel retaining cup according to ASTM (1997c) C 1231.

Freeze–thaw durability

The resistance of mortar beams to deterioration from repeated cycles of freezing and thawing was tested in accordance with ASTM C 666 (ASTM 2003). This standard covers two test variations: Procedure A continuously submerges the beams in water, whereas Procedure B submerges the beams in water only during the thawing cycle. Procedure A is more severe than Procedure B and could have been chosen for this study to accelerate the

damage. However, unless special attention is paid to the type of canister used for housing the beams in Procedure A, ice formed between the canister wall and the beam during testing can damage the beam. Another problem with canisters is that a uniform layer of water should be maintained around the beam throughout the testing. This is difficult to do, especially if the beams change dimensions during testing because of scaling. If the beam is not always centered in the canister, differential pressures, caused by different ice thickness around the beam, will develop. To avoid potential problems associated with canisters, Procedure B was selected for the main part of this study where the beams are frozen in air. (Procedure A was used for the salt-scaling section of this study.) The beams were supported such that they were not in full contact with the bottom of the test chamber. The primary difference between this testing and that outlined in the ASTM standard is that the beams were cured for 28 days rather than the specified 14 days.

The freezing and thawing cycle consisted of alternately cooling the center of each beam from 4 to -18°C in air and by warming it back to 4°C in water. Strict adherence to the ASTM standard requires that the center of each beam be within $\pm 2^{\circ}\text{C}$ of these temperatures at the end of the cooling and heating periods. Further, the time to cool from 3 to -16°C should be at least half of the cooling period, and the time to warm from -16 to 3°C should be at least half of the thawing period. Thawing time should constitute at least 20% of each cycle.

All freezing and thawing was done in a Scientemp Corp. apparatus capable of handling sixty $76.2\text{-} \times 76.2\text{-} \times 304.8\text{-mm}$ concrete beams. Each freeze–thaw cycle was monitored by embedding thermocouples in two dummy beams placed at the far ends of the apparatus. Figure 5 shows a typical set of freezing and thawing cycles. The figure shows that each freeze–thaw cycle ran 3 hours and 9 minutes and essentially satisfied the ASTM requirements mentioned above. The freeze–thaw cycles remained consistent throughout this study, ensuring that each beam was subjected to identical freeze–thaw environments.

The beams were removed from the freeze–thaw apparatus once every 15 to 30 cycles, read for fundamental transverse frequency while in a water-saturated condition, and returned to random positions, turned end-for-end, in the chamber to ensure that each beam was evenly subjected to conditions in all parts of the chamber. Uniformity between cycles was as-

sured by maintaining the chamber at full load capacity by placing dummy beams into empty spaces as needed.

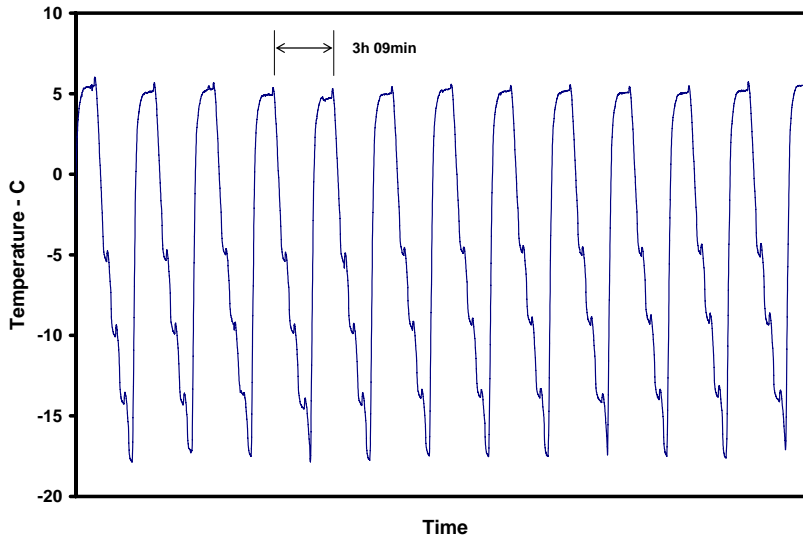


Figure 5. Typical freezing and thawing cycles.

Fundamental frequency

Measuring the change in fundamental frequency assessed the effect of freezing and thawing on the integrity of each beam. The method used in this study is similar to that presented in ASTM C 215 (2002a), which uses an impact resonance apparatus. This study used a Rion Model SA-77 Fast Fourier Transform signal analyzer to display the output from an accelerometer. The accelerometer was a Bruel & Kjaer, Type 4393, high-frequency, low-impedance voltage mode device with a sensitivity of 4.11 mV/g. It weighed 2.5 g and had a resonant frequency of 55 kHz. The operating frequency range was 200 to 15,000 Hz. The accelerometer was attached on the top face of the beam, as close to one end as possible, with a rubber band.

The procedure consisted of causing a beam to vibrate by tapping it lightly with a metal rod, then evaluating the frequency response from the accelerometer. The beam was supported in accordance with ASTM (2002a) C 215 at 22.4% of its length from each end. (Supporting the beam at its nodal points did not appear necessary as supporting it over its entire length on a foam mat produced identical results.) When struck, the beam vibrates at a number of frequencies. The fundamental transverse frequency was identi-

fied as the lowest peak frequency. Frequency measurements were obtained every 15 to 30 freeze–thaw cycles.

Length change

Length changes of the 12.7- × 25.4- × 254-mm mortar beams were measured within a testing chamber fabricated at CRREL. The thinness of the specimens helped to assure that the temperature would remain fairly uniform throughout the cross section of the sample during testing. During the several calibration runs, the largest difference between center and surface temperatures was 10°C.

Figure 6 shows a cutaway drawing of the test chamber and supporting equipment. The chamber consists of a 19-mm-thick plywood box measuring 508 mm W × 508 mm D × 254 mm H, outside dimensions. The box is supported 19 mm above a 25.5-mm-thick aluminum base plate by aluminum blocks placed at its four corners. The inside walls, floor, and top cover of the box are lined with 50.8 mm of extruded polystyrene insulation. In-board of the insulation is a 6.6-mm thick aluminum box, 305 mm W × 248 mm D × 76 mm H, housing the test specimens. A 13-mm air gap separates the aluminum box from the insulation.

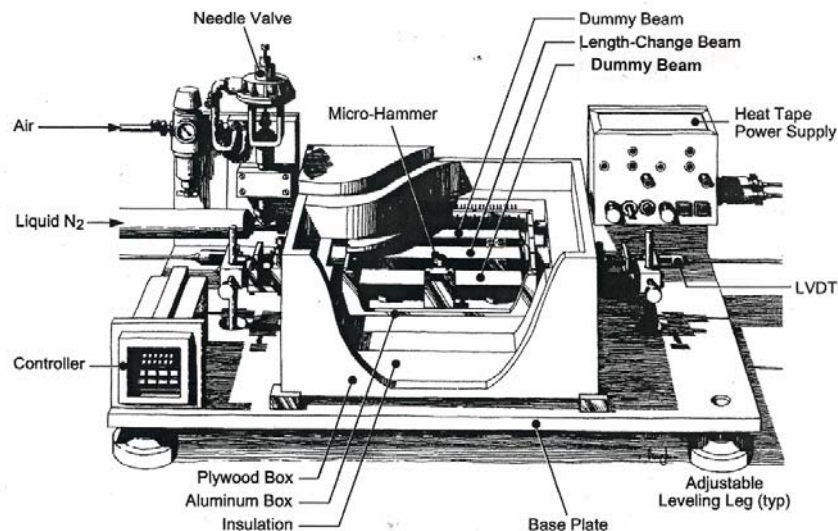


Figure 6. Dilation box.

The chamber is cooled by nitrogen gas that flows in the air gap between the inner aluminum box and the polystyrene insulation that lines the inside of the plywood box. A programmable proportional temperature con-

troller (Omega, Model 2001) regulates the internal chamber temperature by sensing output from a thermistor placed beneath the test beam at its approximate center. The nitrogen flows from ports in an aluminum-finned evaporator behind the aluminum specimen box. Flow is controlled by a needle valve in an insulated 12.7-mm-diameter line connected to a 160-L liquid nitrogen tank and to the evaporator. The Omega controller regulated the opening on the needle valve. The cooling rate was set at 0.5°C/minute for this study.

Length change measurements were made with LVDTs that monitored the movement of two 9.34-mm-diameter rods contacting either end of the test specimen and that protruded out from the test chamber. The rods, which ran inside a 15.5-mm-diameter metal tube, were lightly spring loaded to follow the specimen as it contracted and expanded. The tube was wrapped with heat tape to assure that the rods remained at room temperature along their length. Thus, the measurements recorded by the LVDTs did not have to be adjusted for thermal movement of the rods. As added assurance, the rods were fabricated from Invar of low thermal expansion, 0.9×10^{-6} degrees $^{-1}$. The two LVDTs, Trans-Tek, Series 350, were connected to a data logger, Omnidata, Model 824, set to read every minute. The system accuracy was ± 0.0014 mm.

The ability of the system to faithfully measure length change was demonstrated with an aluminum alloy (6061-T6) of the same dimensions as the mortar beams. Figure 7 shows the length change-versus-temperature curve for the alloy. With the exception of minor perturbations caused by the cooling system turning on and off, it can be noted that the aluminum beam contracted and expanded linearly—the slope representing the thermal coefficient—as it cooled from room temperature to -60°C and warmed back up again. It can also be noted that the cooling and warming curves did not exactly trace each other. This was not viewed as a problem because length measurements were obtained while the beam was changing temperature, and, because the beam was not in thermal equilibrium, length change probably lagged temperature change. A manifestation of this lag is that the slope varied between approximately 19 and 21 ppm/ $^{\circ}\text{C}$ during the cooling phase and between approximately 20 and 23 ppm/ $^{\circ}\text{C}$ during the warming phase. These do not consistently match the value published for the thermal coefficient of expansion, 23.0 ppm/ $^{\circ}\text{C}$ (Lyman 1961), of the alloy. The best agreement occurred at the end of the test when the heater was turned off. The important findings for this study were that

the length-change line plotted nearly linear and that the length change measurements returned to zero. The aluminum beam was tested three times and all three times it produced the same results.

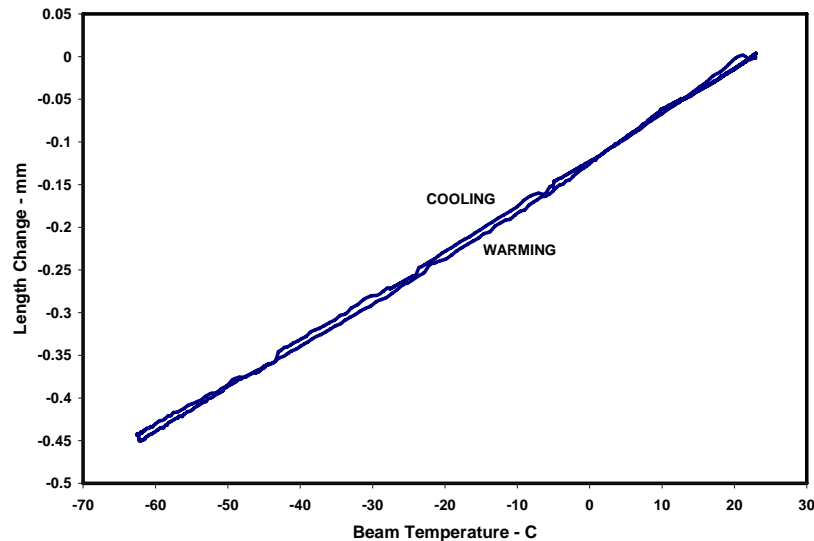


Figure 7. Results of cooling and warming an aluminum beam in the length-change test device.

During testing, three beams were placed inside the specimen box for each test. Two dummy aluminum beams, instrumented with copper-constantan thermocouples at their center of mass, placed near the back and front of the specimen box, were used to estimate the temperature of the test beam during testing. The length-change beam was placed on nylon rollers in the middle of the box. The test beam was supported at approximately the quarter points of its length. The temperature within the aluminum box was fairly uniform, differing only by up to 10°C from front to back—the back usually being cooler.

4 RESULTS AND DISCUSSION

Freezing point

The freezing point—the temperature at which ice first appears in the freshly-mixed mortar—for the 40 mortars containing admixtures, along with the five control mortars, are presented in Table 6. Before we consider the antifreeze mortars, it is interesting to note that the five control mortars all froze at essentially the same temperature. This outcome is not immediately intuitive, as one might expect higher alkali concentrations in lower w/c ratio mixtures and, consequently, lower freezing points. However, it did not seem to matter that the w/c ratio ranged from 0.30 to 0.47, as all control mortars acted alike. What is more, other studies have pointed out, similarly, that mortars (concrete) made without chemical additives typically have one temperature at which nearly all of the mixing water freezes (Mironov 1977). Corroborating this are cooling curves, obtained elsewhere, that show that, once freezing occurs in control mortar, the temperature of the mortar remains constant for an extended period (Korhonen 1999); it does not fall off as shown for the antifreeze mortar in Figure 4. Thus, changing the w/c ratio will not provide increased freeze protection and, once freezing initiates in admixture-free concrete, a high percentage of the mixing water will immediately turn into ice and structural damage is likely.

Table 6. Freezing points (°C) measured at initiation of freezing. Controls are the mortars with no admixtures. All values are the average of measurements from up to three beams.

Admixture concentration* %	Mix 5	Mix 6	Mix 8	Mix 9	Mix 11
0	-1.45	-1.54	-1.41	-1.39	-1.36
1	-1.59	-1.70	-1.60	-1.67	-1.75
3	-1.89	-2.40	-2.08	-2.10	-1.83
6	-3.23	-3.13	-3.14	-3.49	-2.96
9	-3.48	-3.84	-4.04	-4.12	-3.69
12	-4.76	-4.64	-4.96	-4.44	-4.61
16	-6.05	-6.08	-5.82	-5.62	-6.10
20	-8.21	-7.24	-7.59	-7.25	-7.48
24	-9.08	-8.77	-8.29	-8.40	-8.58

* See Table 5 for explanation.

The 40 mortars with antifreeze admixtures froze at temperatures that were lower than those of the control mortars, but not all froze at the same temperature, even though the admixtures were present at the same concentrations in each grouping. Inaccuracies in measuring mixture ingredients, determining aggregate moisture contents, and in the measurement system resolution, explain most of the mix-to-mix variation at each concentration level. Generally, experience has shown that freezing points have been within 0.5°C from each other on a batch to batch basis. Thus, a freezing point measurement, as noted in the Phase I report, can be a good predictor of what is in the mixture. In this study, freezing points served as a quality control measure to assure that the correct dosage of admixture was used in a given mix. It paid off as the wrong dosage was used on one occasion. Figure 8 shows how the freezing point varied with admixture concentration. As can be seen, the freezing point can be approximated as being linearly proportional to the amount of admixture dissolved in the mixing water.

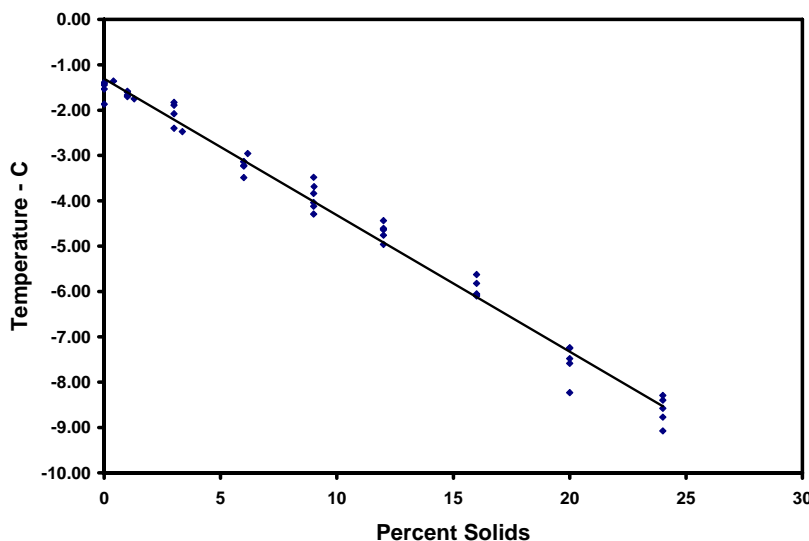


Figure 8. Freezing point versus concentration of solid admixture by weight of water based on Table 6 data plus a few extra confirmatory tests not shown in Table 6. The regression curve is: $Y = -0.3x - 1.3$, where Y = freezing point and x = percent solids.

Strength development

Figure 9 shows the effect of admixture dosage on the ultimate strength of mortar. (Sodium chloride, reagent grade, was used to represent the salts contained in the commercial admixtures because it allowed a precision of measurement not possible with the commercial admixtures, where only

the main ingredients are known in approximate quantities.) As can be seen, mortar becomes progressively stronger with dosage until it reaches approximately 10% by weight of water. Thereafter, the strength drops off as dosages are further increased. To lose strength at higher dosages was expected, as explained earlier, but it was interesting to see that the mortar first became stronger at the lower dosages. We have noted in past studies that some admixtures, particularly accelerators, seem to enhance concrete's ultimate strength. The influence of accelerating admixtures in promoting higher strength is thought to be caused by the chemical reactivity between the cement and the accelerator. Sodium chloride, on the other hand, is not considered an accelerator, yet it too enhances strength. Therefore, it likely has a physical influence on the strength of mortar.

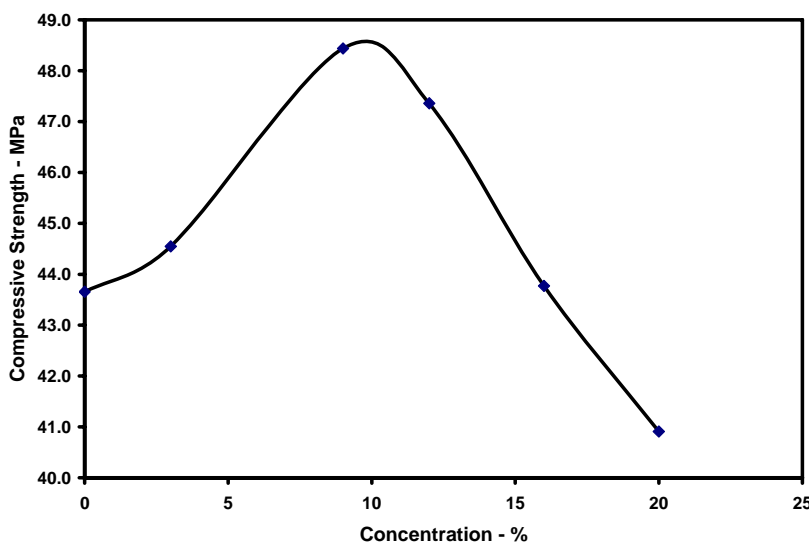


Figure 9. Effect of admixture dosage on the 28-day compressive strength of mix 5 mortar. Sodium chloride served as the admixture in this evaluation.

Goldman and Bentur (1993) offer some insight into this question in their study of silica fume and carbon black. They show that silica fume enhances concrete's strength partly because of the pozzolanic reaction between it and cement. However, their finding that carbon black, which is chemically non-reactive, works nearly as well as silica fume suggests that much of the influence of silica fume is because of a microfiller effect, whereby small particles, with compressive strength of their own, plug the aggregate transition zone voids in concrete, making the concrete stronger. In earlier studies, Sellevold (1982, 1987) found that finely ground rock (calcium carbonate), which is essentially inert, plugs the voids within cement paste,

thereby strengthening the concrete. Thus, the mechanism by which small aggregate-like particles affects concrete's strength is of a physical origin.

Perhaps Figure 9 is showing that sodium chloride has a direct aggregate-like contribution to strength, at least at the lower concentrations. This is said because the strength tests were conducted on air-dried specimens, making it possible that the water-soluble additive recrystallized within the pores of the mortar, whether in the transition zone or the paste matrix, giving it added strength. It could be that the microstructure of the mortar was altered after the admixture dosage reached approximately 10%. However, it is interesting to note that it was not until the admixture concentration rose above 16% that the mortar became weaker than the control. It was outside the scope of this study to explain why admixtures enhance the strength of concrete, so this issue was not pursued any further. We will see later if this drop off in strength has any correlation to freeze–thaw durability.

To this point, the majority of laboratory testing focused on non-air-entrained mixes for reasons explained earlier. The Phase I testing showed that the antifreeze admixtures did not adversely affect the freeze–thaw durability of concrete. However, in keeping with standard practice, whenever field tests were conducted during Phase I, the concrete was entrained with air. In many cases, the air contents of ready-mixed antifreeze concrete was well over the $6 \pm 1.5\%$ specified range—sometimes in excess of 10% air by volume. This was not considered a problem at the time as the air in subsequent batches could be reduced by using less air-entraining admixture. However, for the already dispensed concrete, the strength loss caused by the over abundance of air voids and what effect the extra voids might have on freeze–thaw durability were not addressed in Phase I.

Therefore, a series of tests was conducted in this phase to determine if high air contents pose either a structural or a durability problem. Because only air content was the issue and because air contents were easier to manage in admixture-free concrete, air-entrained control mortar was used in this special study. Figure 10 shows that the compressive strength of mortar is decreased by approximately 5% for each 1% increase in air content, which agrees with the industry rule-of-thumb concerning the influence of air content on the strength of concrete. Because the design strengths of the field-tested concretes in Phase I were greater than necessary, the loss of strength caused by the 10+% air contents were rightly con-

sidered unimportant. The effect of high air contents on freeze–thaw durability is discussed later in this report.

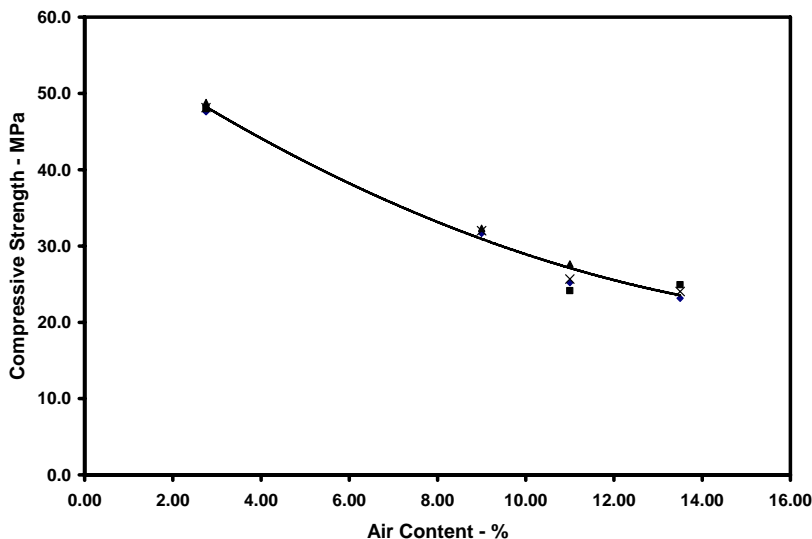


Figure 10. Compressive strength versus air content.

Freeze–thaw resistance

The primary objective of this study was to determine if concrete could be made more durable merely by adding chemicals into the mixing water. To be successful, the chemicals could cause no harm to the concrete or embedded metals and they had to improve concrete's resistance to cycles of freezing and thawing. This study was limited to chemicals that were approved for use as antifreeze admixtures in Phase I. Basically, this assured that no harm could come to the concrete or embedded metals because the chemicals had long ago passed a battery of tests to be approved for use in concrete and have proven in practice to be harmless. Thus, this study needed only to focus on the question of freezing and thawing durability.

The freeze–thaw resistance of the five control and their eight companion antifreeze mortars was determined by subjecting beams to successive cycles of freezing and thawing and assessing the damage by periodically measuring their change in resonant frequency. As the mortar beams deteriorated, both elasticity and resonance frequency decreased. According to ASTM C 666 (ASTM 2003), elasticity and frequency are related as follows:

$$RDME = (n_c^2 / n^2)100$$

where:

- $RDME$ = relative dynamic modulus of elasticity, after C cycles of freezing and thawing
- n = fundamental transverse frequency at zero cycles of freezing and thawing
- n_c = fundamental transverse frequency at C cycles of freezing and thawing.

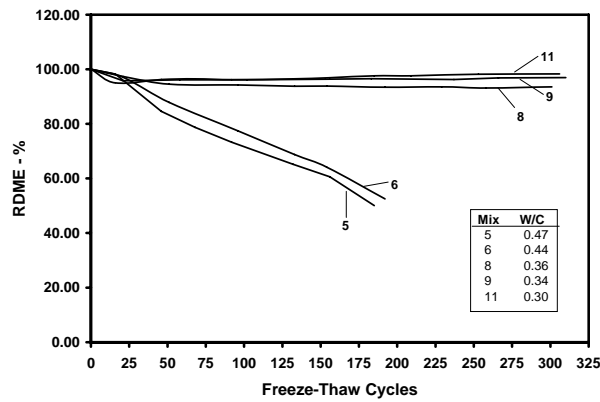
Before the fully cured beams were subjected to freezing and thawing, they were soaked in lime-saturated water for 24 hours and read for fundamental transverse frequency. Frequencies were measured every 15 to 30 freeze–thaw cycles thereafter. ASTM (2003) C 666 considers concrete to be durable if it maintains its $RDME$ above 60% through 300 cycles of freezing and thawing. As mortar is similar to concrete, this guidance was adopted to evaluate the mortar beams in this study.

Figure 11 shows the effect of freezing and thawing on the relative dynamic modulus of elasticity of the 45 mortars.

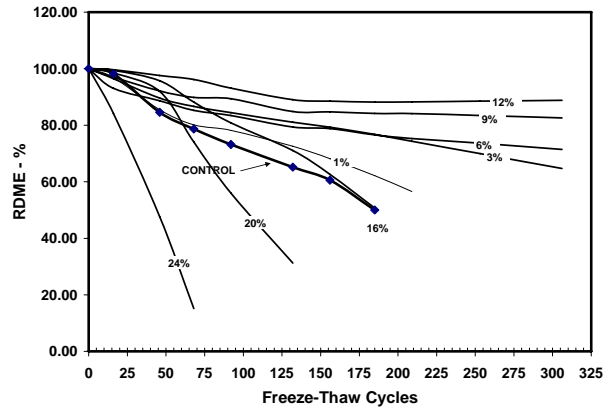
Control mortar

Let us consider only the control mortars for a moment. It is clear that mix 5, the control made with 362 kg/m³ cement, was the least durable of all. It reached 60% of its initial $RDME$ within 150 freeze–thaw cycles, which, according to ASTM (2003) C 666, meant that it was not durable. Likewise, mix 6, the control mortar containing 390 kg/m³ cement, though it lasted more than 165 freeze–thaw cycles before it reached an $RDME$ of 60%, was also not durable. Neither of these two results was unexpected, as all control mortars in this study were non-air-entrained and therefore expected to be non-durable.

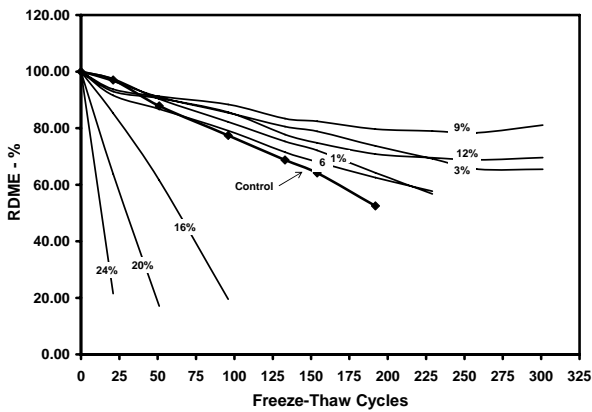
However, the last three control mortars were found to be durable. Mix 8 patterned after concrete containing 474 kg/m³ cement lasted 300 freeze–thaw cycles while its $RDME$ dropped only to 90%. Likewise, mixes 9 and 11 made with 503 and 558 kg/m³ cement, respectively, were even better, dropping to 96 and 98%, respectively, after 300 cycles. These last two control mortars were practically immune to frost damage, even though they contained no entrained air.



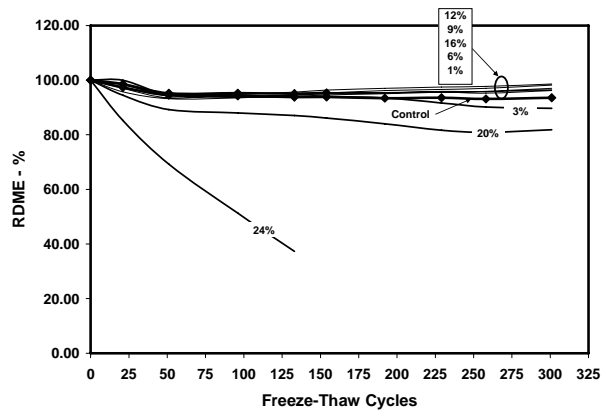
a.



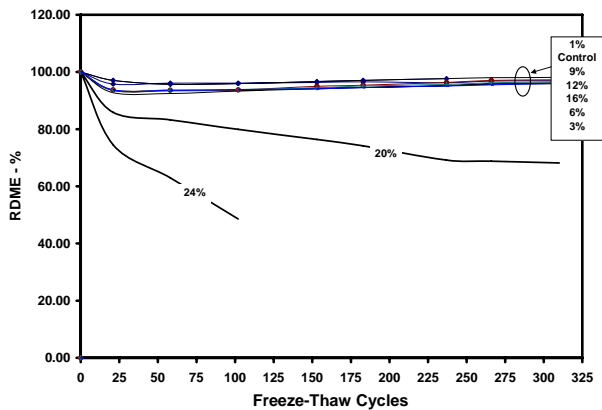
b.



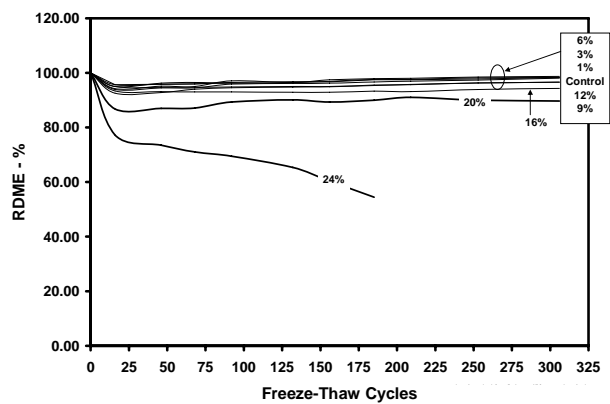
c.



d.



e.



f.

Figure 11. Performance of non-air-entrained mortar subjected to cycles of freezing and thawing. Each line represents the average of three beams. The percentages shown represent the concentration of admixture solids by weight of free water in the mix. Where the lines are closely grouped, the relative position of each line from top to bottom is provided in a textbox. (a-control mortars; b-mix 5; c-mix 6; d-mix 8; e-mix 9; f-mix 11) RDME is relative dynamic modulus of elasticity.

The first observation that one might make is that the amount of cement influenced the results—i.e., as the cement factor increased, so did durability. A closer look at these results suggests that the improved performance of the control samples was more related to w/c ratio. A major dynamic in the durability of cement paste is the w/c ratio. This ratio controls whether and how much capillary porosity develops in hardened cement paste. Capillary pores are voids, created by excess mixing water, that are small enough to absorb water but large enough to readily freeze. As we will see later, the lower the ratio is, the fewer are the capillary pores, which implies less freezable water. Theory suggests that capillary pores are unlikely to form in pastes made with w/c ratios at or below 0.36. The pores that form inside this type of paste are typically so small, gel pores, that water in them will not freeze at ordinary wintertime temperatures. Therefore, cement pastes with w/c ratios below 0.36 should be considerably more durable than pastes with w/c above that value. Interestingly, this is exactly what occurred. Mortars 5 and 6 contained w/c ratios above 0.36 and were accordingly susceptible to frost damage—the higher the w/c ratio was, the earlier the damage occurred. The mortars made with w/c ratios at or below 0.36 experienced minimal frost damage. They, obviously, contained less freezable water compared to the first two control mortars discussed.

Earlier, we saw that the strength of mortar decreased as air content increased. Durability, as shown in Figure 12, was largely unaffected by high air contents—mortars made with 9, 11 and 13.5% air retained full *RDME* after 300 cycles of freezing and thawing. Thus, if winter concrete mixtures used by state DoTs routinely contain more cement than their summertime counterparts, as they seem they do, high air contents should not be a concern for strength or durability.

Antifreeze mortar

For those mortars made with the admixture, durability depended on the amount of admixture used. In general, the admixture significantly improved the durability of the two highly frost-susceptible control mortars, i.e., mixes 5 and 6, when the admixture was used at moderate concentrations. Invariably, durability significantly diminished in all mortars at the highest admixture concentration. As a reference, Figure 8, a relationship between admixture concentration and freezing point, shows that the MB IV admixture should be used at approximately 12% concentration to produce the -5°C freezing point target set in Phase I. Except for Mix 6, Figure 11 shows that the admixture formulation enhances the freeze–thaw dura-

bility of mortar within the range of admixture concentrations used in Phase I—essentially any concentration below 16% provided benefit.

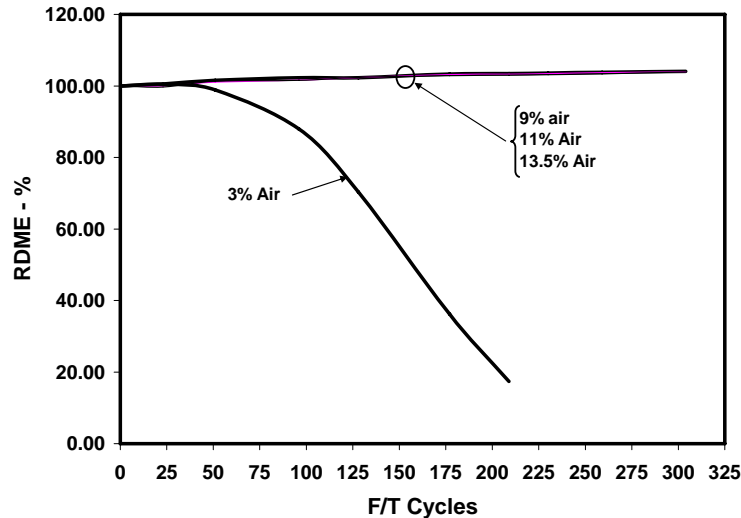


Figure 12. Effect of air content on freeze–thaw durability of four control beams from Mix 5.

Why did the durability of the mortars increase when they contained admixtures? Concerning water contents, there was no difference between the mortars made with admixtures and their corresponding controls. Each had the same w/c ratio. Yet, the mortars made with admixtures behaved as if they had less freezable water than did the controls. It is true that the admixtures depressed the freezing point of the mixing water, but not nearly enough to resist the -20°C temperature of each freeze–thaw cycle. Is it possible that the freezing point of hardened mortar is different from that when it was freshly mixed? Korhonen et al. (1998) investigated the effect of curing time on the freezing point of antifreeze concrete and found that, indeed, the temperature at which ice first appears in concrete decreases with age. They showed that the freezing point of concrete changed from -3.3°C when it was fresh to -8.4°C when it was pre-cured at 20°C for 30 hours before being frozen. During this study several mortars, cured for more than 28 days in lime-saturated water held at 20°C , were measured for their freezing points. As Figure 13 shows, the approximate freezing point of a mortar was -5.8°C when fresh and -17°C when fully cured. (Elsewhere, the freezing point of normal concrete when fully cured was measured to be -4.6°C . [Pierce et al. 1996]) Because the thermal signal from water freezing inside hardened mortar is weaker than that from fresh mortar, it was difficult to identify the marked indications of freezing

shown in Figure 4. Perhaps a highly sensitive calorimeter would yield better results than did our embedded thermocouples. More work is needed.

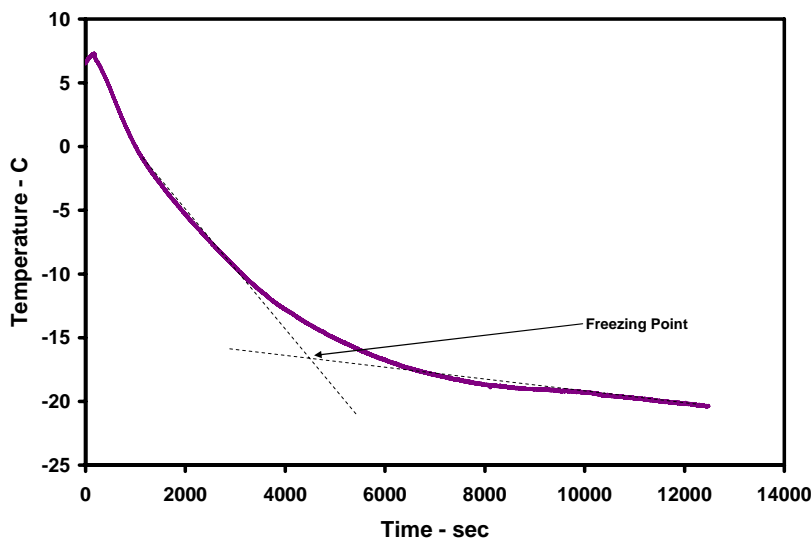


Figure 13. Time-temperature cooling curve used to determine the freezing point (-17°C) of hardened mortar (Mix 8) made with admixture MB IV at 16% concentration by weight of water. When fresh, the freezing point was approximately -5.8°C . A thermocouple embedded within a cylinder of fresh mortar measured the cooling curve at 1-second intervals when the mortar was fully cured. The freezing point is identified as the intersection of projections of the cooling curve and the freezing curve.

Because dissolved chemicals are present in antifreeze mortars, one explanation for the improvement in durability is that admixtures, by depressing the freezing point of water even slightly, caused ice to form more gradually as temperatures drop, whereas, in the controls, nearly all of the water turned to ice at one temperature. A gradual development of ice might allow the paste matrix time to partially elastically accommodate the resulting expansion without the same amount of damage caused by a sudden development of ice. If this occurred, frost damage would be lessened in mortars made with admixtures. As we have already seen, it is also likely that the concentration of admixture in the pore water was higher than that in the original mixing water. The hydration process is known to exclude impurities from the products of hydration, much like what happens when pure ice freezes out of solution. The result is a pore solution that continually increases in concentration and decreases in freezing point as the cement paste matures. In addition, the admixtures left in the pores could make the pores smaller by acting as fillers. Both of these effects would make it more difficult for water to freeze and would make the concrete

more resistant to frost damage. More study is needed to better answer these questions.

If the freezing point of hardened mortar continues to drop with increasing dosages of additive, which should make it increasingly more difficult for water to freeze, why does the durability decline markedly at the higher dosages used in this study? The answer probably is that cement paste, when fully hardened, is not solid but contains numerous pores of various sizes. During hydration, cement chemically combines with water, producing a gel of fixed porosity. Pore structure develops by the gradual growth of gel into space originally occupied by anhydrous cement and mixing water. At w/c ratios above 0.36, the gel cannot fill all available space, so the porosity of hardened cement paste becomes part that of the gel plus that of the water-filled space not filled by gel. The unfilled water spaces are called capillaries and, accordingly, the porosity of hydrated cement paste consists of gel and capillary pores, of which there are a finite amount, depending on the cement factor and amount of water used in a given mix.

Thus, only so much chemical can be added into a mix before there is more of it than pore space can accommodate. Interestingly, Mix 5 held up to 16% admixture by weight of water (7.5% by weight of cement) before its strength (Fig. 9) and durability (Fig. 11b) dropped to equal that of the control mortar. Moreover, Mix 11 was rated freeze–thaw durable (Fig. 11f) when it contained 20% admixture by weight of water or 6% admixture by weight of cement. Thus, the freeze–thaw durability of antifreeze mortar appears to be strongly tied to the amount of cement used in its mix design (e.g., mixes 9 and 11 contained the most cement and performed the best in freeze–thaw testing). Until more tests are conducted, no more than 7.5% admixture (by weight of cement) should be used to make antifreeze concrete.

Though a plausible explanation has been forwarded for the effect of admixture concentration on the freeze–thaw durability of concrete, the microstructure of antifreeze concrete should now be studied in greater detail to confirm these assumptions.

Length change of mortar bars

Concrete, upon freezing, is considered to be susceptible to frost action if it dilates and to be immune to frost action if it does not dilate. Because even frost-resistant beams usually dilate somewhat, it has always been a judg-

ment call as to how much dilation signals frost-susceptibility. Presumably, if dilation occurs at all, the deterioration process has begun and the material will eventually fail with repeated cycles of freezing and thawing. And, obviously, large dilations would lead to quicker failure than small dilations. However, if a beam dilates during freezing and returns to its original length upon thawing, could frost damage have occurred? We will explore this question later on.

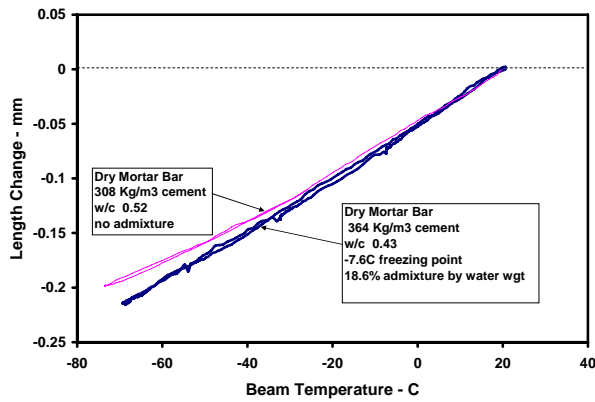
The length-change test recorded the contraction and expansion of mortar beams cooled from room temperature to -60°C and below and warmed back up again. Length-change curves for each of the five mixes made with and without admixtures are presented in Figure 14 and Appendix C.

Control Mortar

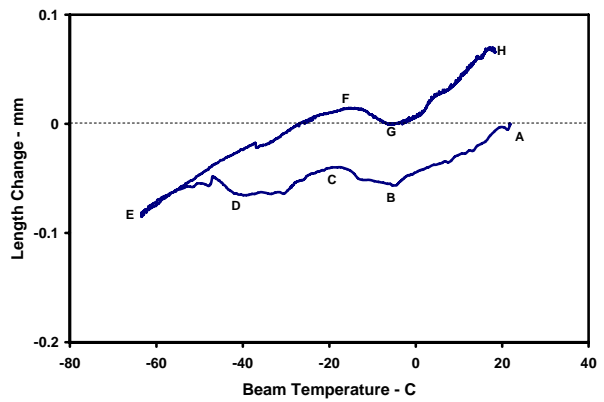
Figure 14 presents the length-change curves from water-saturated control beams. For comparison, Figure 14a illustrates a typical result from an oven-dry control and an antifreeze beam. Both dry beams contracted and expanded more or less linearly with temperature and returned to their original lengths at the end of the test. Though these results illustrate the obvious, that dry concrete is unaffected by freezing and thawing because there is no water present to cause expansion, they provide important benchmarks for the rest of the test results.

It is clear in Figures 14b and 14c that mixes 5 and 6 behaved differently from the last three control beams. The length-change curves of the beams made from mixes 5 and 6 exhibited a pronounced hysteresis between cooling and warming. They consisted of seven distinct regions, labeled in Figure 14b, while control beams made from mixes 8, 9, and 11 tended to return to their original lengths. The following discussion applies to the seven regions of the length-change curves for the beams made from mixes 5 and 6.

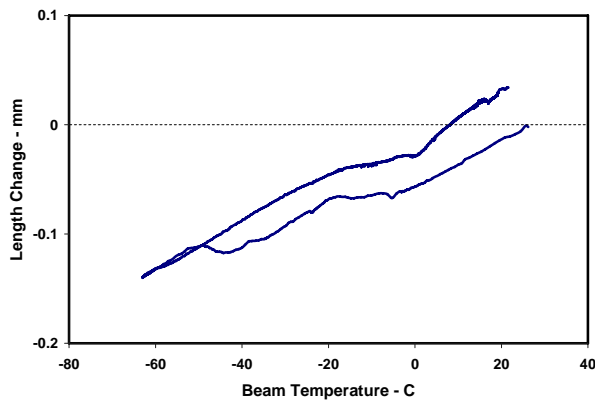
On cooling between 20 and -5°C (region AB), both beams contracted linearly at approximately $8\text{ ppm}/^{\circ}\text{C}$, which compares favorably to published values for the thermal coefficient of expansion of mortar of between 7 and $12\text{ ppm}/^{\circ}\text{C}$ (Mindess and Young 1981, p. 526). In fact, all beams in this study behaved similarly in this region, including the two oven-dry mortars in Figure 14a, which contracted at rates between 9 to $10\text{ ppm}/^{\circ}\text{C}$. Thus, all length changes measured in this region are considered thermally induced.



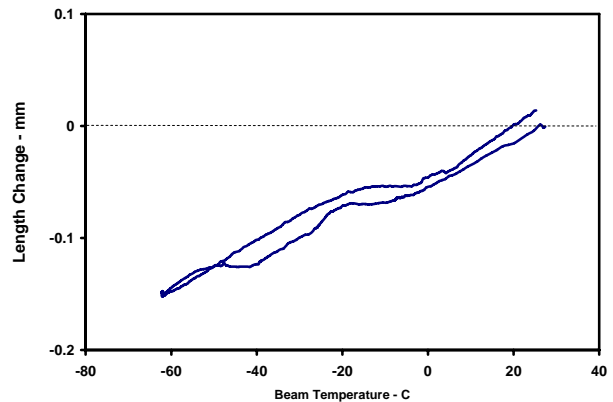
a.



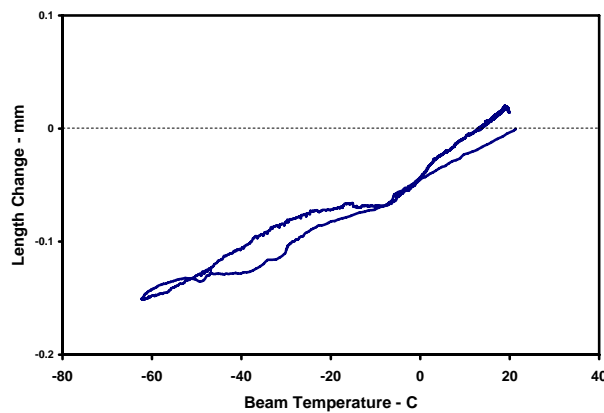
b.



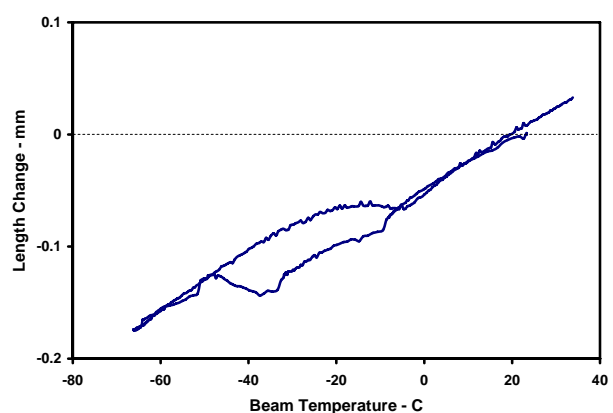
c.



d.



e.



f.

Figure 14. Length-change curves for non-air-entrained control mortar beams subjected to cooling cycle. (a—oven-dry control and antifreeze mortar; b—mix 5; c—mix 6; d—mix 8; e—mix 9; f—mix 11.)

In region BC, between approximately -5 and -20°C , both beams expanded. Some of this expansion is caused by water turning into ice inside the large capillary pores. This is noted as a sudden increase in length of each beam. The temperature at which ice first forms is considered the freezing point of the mortar. In support of this contention, Pierce et al. (1996) measured the freezing point of mature concrete to be -4.6°C . After the initial rapid expansion, both beams continued to expand at a slower rate. Most likely, this secondary expansion is caused by water migrating from smaller pores to the bulk ice. This accreting of ice in limited spaces added to expansive stress and slower continued expansion of the beams.

In region CD, most of the large capillary pores have frozen and water from the small pores continues to migrate to the locations of the bulk ice. This is equivalent to drying and is manifested as shrinkage. Thus, there are three processes occurring between approximately -20 and -40°C : thermal contraction of the matrix, drying shrinkage of the small pores, and ice build up in the coarse pores. The net effect is contraction, though at a lower rate than the one at which it initially started out.

In region DE, at approximately -40°C , the two control beams expand for a second time. It is apparent that water in the smaller pores, rather than just migrating to the bulk ice, has begun to freeze in place and generate its own hydraulic stress. Though interesting, the extra frost damage between -40 and -60°C occurs at temperatures to which concrete structures are seldom exposed. Therefore, the expansion in DE is of little practical significance, unless the concrete is situated in the deep arctic or used to contain cryogenic liquids.

On warming—region EF—the beams expand. One might expect the beams to contract as ice in the smallest pores begins to melt and reduce in volume. However, the expansion of the mortar matrix in this region closely resembles the thermal coefficient measured in region AB. A possible explanation for this expansion could be that the unmelted ice in the coarse pores and the cement paste is thermally expanding, as it should as it warms, to counteract the decrease in volume of ice in the small pores, so the net effect is the thermal expansion of the mortar matrix itself. It is also possible that the water that diffused from the small gel pores migrates back during thawing. It is not clear what mechanism is causing the mortar to lengthen in this region. It is clear, however, that each of the two control mortars significantly expanded between approximately -60 and -20°C .

Melting of the ice in the larger pores causes the mortar to contract in FG. In this region, all of the small pores have melted and reabsorbed water. The tensional force in the water in the small pores is largely reduced. Thus, the volume change of ice to water is the direct cause of the contraction measured between -20 and 0°C .

At 0°C all ice has melted and normal thermal expansion once again predominates between 0 and 20°C .

It is significant to note that neither of the two control mortars returned to their original length when warmed back up to room temperature. This implies that neither mortar is immune to frost action, which is supported by the freeze–thaw results presented in Figure 11—both beams failed in less than 175 cycles of freezing and thawing.

In contrast, the control beams made from mixes 8, 9, and 11 were highly frost resistant. They showed little sign of deterioration at the end of 300 freeze–thaw cycles. The w/c ratio used to make these mortars helps to explain the differences in durability among the control beams.

The primary influence of w/c ratio on the freeze–thaw durability of mortar is its effect on capillary pore volume. Provided that the w/c ratio is below 0.36, the pore structure of the cement paste within mortar consists primarily of gel pores. Above this ratio, relatively large capillary pores, caused by excess water not needed for cement hydration, begin to appear—the more water, the greater the capillary pore volume (Powers and Brownyard 1946–47). The freezing point of water within hardened paste depends on the diameter of the pore in which it is entrapped. For example, water in pore diameters of $10\ \mu\text{m}$ will not turn to ice until -5°C , in pore diameters of $3.5\ \mu\text{m}$ until -20°C , and in pore diameters of $0.0033\ \mu\text{m}$ until -40°C . Mehta (1986) showed that the pore size distribution in cement paste ranges from $10\text{--}0.02\ \mu\text{m}$ for capillary pores to $0.01\text{--}0.0005\ \mu\text{m}$ for gel pores. Clearly, only capillary pores, which are dependent on w/c ratio, and the larger gel pores, which are independent of w/c ratio, can freeze at ordinary winter temperatures.

Figure 14, besides indicating when water freezes in mortar, provides insight into the predominant size of pores within a mortar. Specifically, because mixes 5 and 6 expanded at approximately -5°C , we can say that they contained a significant amount of capillary pores around $10\ \mu\text{m}$ and that

their w/c ratio was probably above 0.36. Table 4 confirms this. Mix 8 (Fig. 13d) contracted linearly until approximately -20°C when it expanded for the first time. This event suggests that the predominant pore size may be around $3.5\ \mu\text{m}$. Mixes 9 and 11 (Fig. 13e and f), which first expanded at approximately -40°C , suggests a finer pore structure centered at $0.0033\ \mu\text{m}$.

Though mixes 8, 9, and 11 proved highly frost-resistant in the freeze–thaw tests, they did not trace a linear line throughout the cooling and warming cycle, which would have been a clear indication that they were immune to frost damage. The explanation for this apparent discrepancy is that the length-change test cycled beams to lower temperatures than did the freeze–thaw tests. The lower temperatures froze water in pores that would otherwise have remained unfrozen. If the length-change test was limited to the -20°C used in the freeze–thaw testing, it is expected that the curves for these mortars would have been linear.

Antifreeze Mortar

Interestingly, the antifreeze beams generally showed larger changes in length (Appendix C) over the entire thermal cycle than did their respective controls (Fig. 14). However, many of these changes occurred below -20°C . Perhaps the most useful indicator of each beam's resistant to frost damage, and, thus, the best comparison to the freeze–thaw test results, is the temperature at which they first began to expand.

Table 7 was produced by estimating the temperature where each beam first noticeably expanded, which in most cases can be considered the freezing point. Generally, the freezing point drops as the admixture concentration increases and as the w/c ratio decreases. However, the freezing point appears to reverse itself and begin to increase at some of the higher admixtures concentrations. This is not considered possible as freezing points should continue to decrease as concentration increases. Rather, as noted earlier, there is only a certain amount of admixture that can fit into the void spaces within mortar. Therefore, it is felt that the apparent drop-off in freezing point is the signal that the mortar has been saturated with admixture and that freeze–thaw durability could be compromised.

Table 7. Temperature, estimated to the nearest degree Celsius, that mortar beams first began to expand.

Concentration* (%)	Mix 5	Mix 6	Mix 8	Mix 9	Mix 11
0	-5	-5	-17	-40	-38
1	-5	-13	-40	-35	-38
3	-11	-15	-40	-37	-32
6	-13	-40	-40	-37	-40
9	-17	-38	-40	-38	-34
12	-26	-15	-40	-30	-33
16	-10	-7	-12	-35	-32
20	-9	-5	-9	-12	-31
24	-10	-5	-7	-20	-13

*Concentration is based on the weight of solids added by the admixture into the total weight of free water in the mortar.

Therefore, mix 5 (Table 7) should become increasingly more freeze–thaw durable as admixture concentration increases, until it reaches 12%; then durability should begin to decline. This agrees with the freeze–thaw results in Figure 11. Likewise, based on Table 7, the optimum admixture concentrations for the rest of the beams are: 9% for mix 6; 12% for mix 8; 16% for mix 9; and 20% for mix 11. (The w/c ratios presented in Table 4 can be used to convert these percents based on water content to percents based on cement content if desired.) Thus, as the w/c ratio is decreased, the dosage of admixture, based on cement content, can either be decreased to maintain the freeze protection level or the dosage can be kept constant to increase the freeze protection level without compromising durability. And finally, it is apparent that the addition of admixtures to the mortar creates a mortar that can be highly resistant to frost damage, even without it being entrained with air.

Salt scale

The testing thus far has evaluated the performance of mortar exposed to cold air. In these tests, freezing progresses in stages: partly because of a steady increase in the concentration of the admixture in water that has not yet frozen, and partly because the freezing point of water decreases with pore size. Two mechanisms cause frost damage. First, when water turns to ice, the resulting 9% volume increase forces excess water to flow out of saturated pore cavities. The hydraulic pressure developed can be sufficient to overstress the mortar. The second destructive force in mortar is caused

by diffusion of water flowing toward areas of higher solute concentrations brought about by the separation of pure ice from solution. It is generally acknowledged that a slab freezing from the outside inward will scale if fresh water has access to the slab from the bottom and travels upward through the slab by osmotic pressure.

Osmotic pressure is thought to intensify when deicers are applied to concrete surfaces, such as roads and bridges, and become absorbed by the top layer of the structure. This situation is believed to create a higher osmotic pressure than normal where ordinary pore water, containing low concentrations of dissolved alkalis, from within the structure moves outward toward a freezing front that now contains relatively high concentrations of deicer. When the osmotic pressure in the concrete exceeds its tensile strength, scaling damage occurs. The extent of damage varies from minor surface scaling to delamination of large layers of concrete. Generally, the colder the climate is, the worst is the salt scaling damage.

This test evaluated the effect of freezing and thawing mortar specimens in salt water in accordance with ASTM (2203) C 666, Procedure A. The salt water, which contained 4 g of anhydrous calcium chloride per 100 g of tap water, simulated the application of deicer salt by surrounding specimens throughout each freezing and thawing cycle. The most frost-susceptible mix, mix 5, was used in this study. At the age of 28 days of curing, the beams were submerged in tap water 24 hours before testing began.

Table 8. The number of freeze–thaw cycles before specimens made from Mix 5 reached 60% *RDME* (based on Fig. 15).

Test Condition	Concentration* (%)					
	0	3	9	12	16	20
ASTM Procedure B	158	>300	>300	>300	165	85
ASTM Procedure A w/ salt solution	47	75 (estimated)	47	65	27	17

* Weight of solid portion of admixture divided by weight of free water in mortar mixture times 100.

Figure 15 shows the changes in relative dynamic modulus of elasticity as a function of freeze–thaw cycle in a salt solution for mortar containing various concentrations of admixture. In comparison to Figure 11b, which tested companion specimens without salt solution, it can be seen that the moderate dosages of the admixture improved mortar’s freeze–thaw performance, as measured by *RDME*. However, as Table 8 shows, the overall performance of the beams was greatly reduced when they were exposed to

deicer salts. Visually, the outer surface of the beams exposed to the deicer appeared more scaled and pitted than the beams not exposed to the deicer during freeze–thaw testing.

While the scope of the testing in this section of the report is too limited to permit specific conclusions about the frost resistance of mortar in salt water, it can be concluded that moderate dosages of admixture should not create a less durable concrete compared to control. A recent inspection of bridge repairs made with antifreeze and control concrete agrees with this conclusion as shown in Figure 16.

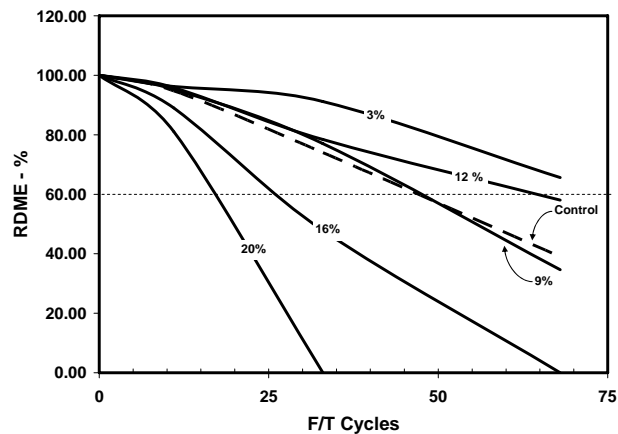


Figure 15. Effect of using saltwater to surround beams during freeze–thaw testing control and antifreeze concrete made from mix 5. The percentages represent the concentration of solids from the admixtures by weight of free water in the mix.



a. Control section.



b. Antifreeze section.

Figure 16. Visual survey of bridge repair after exposure to two New England winters.

5 SUMMARY AND CONCLUSIONS

During Phase I, it eventually became evident that admixtures, besides helping to extend the construction season, enhanced the frost resistance of concrete. At first this finding was questioned, as other researchers have shown that various chemicals, including sodium chloride (table salt), often led to frost scaling. However, a closer look at their data revealed that scaling damage was at its worst when concrete was exposed to chemical solutions of around 5% concentration. It appeared that high admixture doses might be beneficial to the long-term performance of concrete in a cold region. The preponderance of research on the freeze–thaw durability of concrete has largely been directed at improving physical microstructure of concrete and little, if any, attention has been directed at possible benefits of altering the pore water chemistry of concrete by using admixtures. Thus, Phase II of this study addressed the effect of high doses of the chemical admixtures used in Phase I on the freeze–thaw resistance of mortar.

Though mortar instead of concrete was used in this study, all conclusions are considered valid for concrete. The primary conclusion from this study is that admixtures, when used in moderate dosages, can improve the freeze–thaw durability of concrete. The conclusions supporting this are shown below.

1. It appears that the freeze–thaw durability of concrete increases with admixture dosage until its paste pore volume is filled with admixture.
2. The freezing point of mature antifreeze concrete can be lower than when it was freshly mixed and significantly lower than that of mature normal concrete. Thus, concrete made with antifreeze admixtures can be expected to experience fewer freeze–thaw cycles than normal concrete, and, as a result, last longer than normal concrete in northern climates.
3. In the length-change test, the temperature at which concrete beams first expanded—the freezing point of hardened concrete—progressively declined as admixture dosage increased for all moderate dosages. This supports the conclusion put forth above that the freezing point of mature concrete is lower than that of fresh concrete and that it decreases as admixture dosage increases.

4. At the high admixture dosages in the length-change test, the behavior of the beams changed. Rather than continuing to expand at progressively lower temperatures, they began to expand at higher temperatures as dosages increased. This suggested that the concrete was becoming more susceptible to frost damage.
5. The dosage of the MB IV admixture at which the freeze–thaw durability of antifreeze concrete becomes equal to that of control concrete appears to be around 7.5 % of the weight of cement in the concrete. Below this approximate value, durability is enhanced and above it durability is decreased compared to control concrete.
6. The dosage of the MB IV admixture required to protect fresh concrete against freezing down to -5°C is around 12% by weight of free water in the concrete mixture.
7. The freeze-protection limit for freeze–thaw durable concrete can be lower than the -5°C limit set in Phase I.

6 NEEDED RESEARCH

It is clear from the Phase I study that the winter construction season can be extended by using commercial admixtures to depress the freezing point of water and accelerate the hydration rate of cement in concrete. Phase II expanded this finding by showing that the freeze–thaw durability, and thus the service life, of concrete can also be enhanced by using the admixtures studied in Phase I. What is not fully understood is how these or other chemicals affect these changes. The following recommendations are made concerning future research:

- Measure the freezing point of maturing and matured antifreeze concrete. Because the concentration of admixture in the mixing water increases as the cement hydrates, it is important to know how the level of freeze protection changes as a function of concrete age. This new information will help to determine when concrete becomes self-protected against all weather as it cures and if it will become immune to frost damage after it has hardened.
- Measure pore size distribution as a function admixture concentration and w/c ratio. This will define if there is a filling effect to admixtures.
- Extend freeze–thaw cycle testing to at least 1000 cycles to determine if non-air-entrained concrete becomes truly immune to frost damage because of the admixtures. Comparisons should be made to control concrete that contains entrained air.
- Determine if fewer admixtures could be used to extend service life of concrete. Is it permissible to let some ice form within concrete? These data could make antifreeze admixture more cost-effective.

7 REFERENCES

- ASTM. 1987. C 305-82, Standard practice for mechanical mixing of hydraulic cement pastes and mortars of plastic consistency. In *Annual Book of ASTM Standards*, volume 4.01. West Conshohocken, Pennsylvania: American Society for Testing and Materials.
- ASTM .1989. C 109-88, Standard test method for compressive strength of hydraulic cement mortars (using 2-in. or 50-mm cube specimens). In *Annual Book of ASTM Standards*, section 4, volume 4.01. West Conshohocken, Pennsylvania: American Society for Testing and Materials.
- ASTM. 1997a. C 33-86, Standard specification for concrete aggregates. In *Annual Book of ASTM Standards*, section 4, volume 4.02. West Conshohocken, Pennsylvania: American Society for Testing and Materials.
- ASTM. 1997b. C 39-96, Standard practice for compressive strength of cylindrical concrete specimens. In *Annual Book of ASTM Standards*, section 4, volume 04.02. West Conshohocken, Pennsylvania: American Society for Testing and Materials.
- ASTM. 1997c. C 1231-93, Standard test method for compressive strength of cylindrical concrete specimens. In *Annual Book of ASTM Standards*, section 4, volume 04.02. West Conshohocken, Pennsylvania: American Society for Testing and Materials.
- ASTM. 2002a. C 215-02, Standard test method for fundamental transverse, longitudinal and torsional frequencies of concrete specimens. In *Annual book of ASTM Standards*, section 4, volume 04.02. West Conshohocken, PA: American Society for Testing and Materials.
- ASTM. 2002b. C 150-02a, Standard specification for portland cement. In *Annual Book of ASTM Standards*, section 4, volume 4.02. West Conshohocken, Pennsylvania: American Society for Testing and Materials.
- ASTM. 2003. C 666/C 666M-03, Standard test method for resistance of concrete to rapid freezing and thawing. In *Annual Book of ASTM Standards*, Section 4. West Conshohocken, Pennsylvania: American Society for Testing and Materials.
- ASTM. 2205. C 1622, Standard Specification for Cold-Weather Admixture Systems. In *Annual Book of ASTM Standards*. West Conshohocken, Pennsylvania: American Society for Testing and Materials.
- Fagerlund, G. 1997. Scaling, absorption, and dilation of cement mortars exposed to salt/frost. In *Freeze-Thaw Durability of Concrete*. London: E&FN Spon.
- Goldman A., and A. Bentur. 1993. Influence of microfillers on enhancement of concrete strength. *Cement and Concrete Research* 23(4): 962–972.

- Grapp, A. A., V. B. Grapp, and A. S. Kaplan. 1975. The structure and cold resistance of concretes containing antifreeze admixtures [in Russian]. In *Proceedings of the 2nd International Symposium on Winter Concreting, 14–16 October*. Vol. 1. Moscow: Stroyizdat, 60–68.
- Korhonen, C. J. 1999. Expedient low-temperature concrete admixtures for the Army, Special Report 99-17. USA Cold Regions Research and Engineering Laboratory.
- Korhonen, C. J., and A. A. Jeknavorian. 2005. Breaking the freeze barrier. *Concrete International* 27(11): 38–43.
- Korhonen, C. J., J. Hughes, F. Best, and G. Mass. 1998. Low-temperature repair of the ice condenser floor slab at the Sequoyah Nuclear Power Plant. In *Proceedings, 9th International Conference on Cold Regions Engineering, 27–30 September 1998, Duluth, Minnesota*.
- Korhonen, C. J., P. M. Semen, and L. A. Barna. 2004. *Extending the Season for Concrete Construction and Repair: Phase I—Establishing the Technology*. ERDC/CRREL TR-04-02. Hanover, NH: U.S. Army Engineer Research and Development Center.
- Kukko, H., and I. Koskinen. 1988. *RILEM recommendations for concreting on cold weather*. Research Note 827. Technical Research Centre of Finland (VTT), Concrete and Silicate Laboratory.
- Litvan, G. G. 1976. Frost action in cement in the presence of de-icers. *Cement and Concrete Research* 6: 351–356.
- Lyman, T. (Ed.). 1961. *Metals Handbook*. Volume 1. *Properties and selection of metals*. Metals Park, Ohio: American Society for Metals.
- Mehta, P. K. 1986. *Concrete: Structure, Properties and Materials*. New York: Prentice-Hall.
- Mindess, S. and J. F. Young. 1981. *Concrete*. Englewood Cliffs, New Jersey: Prentice-Hall, Inc.
- Mironov, S. A. 1977. Theory and methods of winter concreting. USA Cold Regions Research and Engineering Laboratory, Draft Translation 545.
- Pierce, P. C., J. J. Mieczkowski, E. J. Gannon, and C. J. Korhonen. 1996. Reconstruction of Windsor Bridge piers. *Transportation Research Record* No. 1544, *Materials and Construction*. Washington, DC: National Academy Press.
- Pigeon, M., R. Pleau, and P.C. Aitcin. 1986. Freeze-thaw durability of concrete with and without silica fume in ASTM C 666 (Procedure A, Test method: Internal cracking versus scaling). *Cement, Concrete, and Aggregates*, 8(2): 76–85.
- Powers, T. C., and T. L. Brownyard. 1946–47. Studies of the physical properties of hardened portland cement paste—Parts 1–9. *Journal of the American Concrete Institute* 15(2–8).
- Sellevoid, E. J. 1982 and 1987. Personal communication with C. J. Korhonen, U.S. Army Cold Regions Research and Engineering Laboratory.

- Sellevoid, E. J., and T. Farstad. 1991. Frost/salt testing of concrete: Effect of test parameters and concrete moisture history. *Nordic Concrete Research*, 10: 121–138.
- Verbeck, G. J., and P. Klieger. 1957. *Studies of "salt" scaling of concrete*. Bulletin 150. Washington, DC: Highway Research Board, 1–13.
- Whiting, D., and D. Stark. 1983. *Control of air content in concrete*. National Cooperative Highway Research Program Report 258. Washington, DC: Transportation Research Board.

APPENDIX A: Batch proportions

ID	Admixtures				Sand				Water		Cement	Comments
	Amount to add		Water in admix		Net ssd (g)	Abs (%)	MC (%)	To Add Wgt (g)	Net (g)	To Add (g)	To Add (g)	
Mix/% solids	RC-CNI (g)	P20+ (g)	RC-CNI (g)	P20+ (g)								
	sg=1.295 % solid 32.5	sg=1.35 % solid 40.0	A	B	C	D	E	F	G	H	I	
5/0					10251.1	1.1	.11	10149.6	2050.8	2152.3	4363.5	w/c = 0.47
5/1	25.92	30.67	17.49	18.40	10251.1	1.1	.11	10149.6	2050.8	2116.41	4363.5	
5/3	75.39	92.01	50.89	55.20	10251.1	1.1	.11	10149.6	2050.8	2046.21	4363.5	
5/6	150.78	184.01	101.78	110.41	10251.1	1.1	.11	10149.6	2050.8	1940.11	4363.5	
5/9	226.17	279.85	152.66	167.91	10251.1	1.1	.10	10148.6	2050.8	1832.73	4363.5	
5/12	301.56	371.86	203.55	223.12	10251.1	1.1	.10	10148.6	2050.8	1726.63	4363.5	
5/16	400.51	494.54	270.34	296.72	10251.1	1.1	.10	10148.6	2050.8	1586.24	4363.5	
5/20	504.17	617.21	340.31	370.32	10251.1	1.1	.10	10148.6	2050.8	1442.67	4363.5	
5/24	605.47	739.89	408.69	443.93	10251.1	1.1	.11	10149.6	2050.8	1299.68	4363.5	
TOTAL	2289.97	2810.04			92259.9				18457.2		39271.5	
	0.47 gal	0.55 gal			203.4 lb				40.69 lb		86.6 lb	
$g/453.59 \times 1/8.33 \times 1/sg^* = gal \quad lb = g/1000 \times 2.20462 \quad 453.59 g = lb \quad F = C \times [1 + (E - D)/100] \quad H = G - [A + B] - [F - C]$												

* Specific gravity.

ID	Admixtures				Sand				Water		Cement	Comments
	Amount to add		Water in admix		Net ssd (g)	Abs (%)	MC (%)	To Add Wgt (g)	Net (g)	To Add (g)	To Add (g)	
Mix/% solids	RC-CNI (g)	P20+ (g)	RC-CNI (g)	P20+ (g)								
	sg=1.295 % solid 32.5	sg=1.35 % solid 40.0	A	B	C	D	E	F	G	H	I	Glenium: sg=1.08; % sol- ids=30
6/0					9815.8	1.1	.18	9725.5	2065.7	2156	4694.7	w/c = 0.44
6/1	22.65	33.0	15.29	19.80	9815.8	1.1	.18	9725.5	2065.7	2129.91	4694.7	6.6 g Glenium 3000 NS
6/3	67.96	98.99	45.87	59.39	9815.8	1.1	.13	9720.6	2065.7	2055.64	4694.7	6.6 g Glenium 3000 NS
6/6	140.45	193.85	94.80	116.31	9815.8	1.1	.13	9720.6	2065.7	1949.79	4694.7	6.6 g Glenium 3000 NS
6/9	212.94	292.84	143.73	175.71	9815.8	1.1	.15	9722.5	2065.7	1839.56	4694.7	6.6 g Glenium 3000 NS
6/12	285.43	387.71	192.66	232.62	9815.8	1.1	.15	9722.5	2065.7	1733.72	4694.7	6.6 g Glenium 3000 NS
6/16	376.04	591.69	253.83	311.82	9815.8	1.1	.10	9717.6	2065.7	1598.25	4694.7	6.6 g Glenium 3000 NS
6/20	475.71	647.55	321.11	388.53	9815.8	1.1	.10	9717.6	2065.7	1454.26	4694.7	6.6 g Glenium 3000 NS
6/24	570.86	775.41	385.33	465.25	9815.8	1.1	.11	9718.6	2065.7	1312.32	4694.7	6.6 g Glenium 3000 NS
TOTAL												
$\frac{g}{453.59} \times 1 / 8.33 \times 1 / sg^* = gal \quad lb = \frac{g}{1000} \times 2.20462 \quad 453.59 g = lb \quad F = C \times [1 + (E - D) / 100] \quad H = G - [A + B] - [F - C]$												

* Specific gravity.

	Admixtures				Sand				Water		Cement	Comments
ID	Amount to add		Water in admix		Net ssd (g)	Abs (%)	MC (%)	To Add Wgt (g)	Net (g)	To Add (g)	To Add (g)	
Mix/% solids	RC-CNI (g)	P20+ (g)	RC-CNI (g)	P20+ (g)								
	sg=1.295 % solid 32.5	sg=1.35 % solid 40.0	A	B	C	D	E	F	G	H	I	Glenium: sg=1.08; % sol- ids=30
8/0					9017.4	1.1	.11	8928.13	2041.2	2130.47	5669.9	w/c = 0.36
8/1	22.65	34.87	15.29	20.92	9017.4	1.1	.11	8928.13	2041.2	2094.26	5669.9	6.6 g Glenium 3000 NS
8/3	54.37	109.59	36.70	65.75	9017.4	1.1	.14	8930.83	2041.2	2025.32	5669.9	6.6 g Glenium 3000 NS
8/6	126.85	204.23	85.63	122.54	9017.4	1.1	.14	8930.83	2041.2	1919.6	5669.9	6.6 g Glenium 3000 NS
8/9	190.29	308.84	128.44	185.31	9017.4	1.1	.13	8929.93	2041.2	1814.9	5669.9	6.6 g Glenium 3000 NS
8/12	249.18	413.45	168.20	248.07	9017.4	1.1	.13	8929.93	2041.2	1712.4	5669.9	6.6 g Glenium 3000 NS
8/16	335.27	547.95	226.30	328.77	9017.4	1.1	.14	8930.83	2041.2	1572.7	5669.9	6.6 g Glenium 3000 NS
8/20	416.82	682.44	281.35	409.47	9017.4	1.1	.14	8930.83	2041.2	1436.95	5669.9	6.6 g Glenium 3000 NS
8/24	498.37	821.92	336.40	493.15	9017.4	1.1	.14	8930.83	2041.2	1298.22	5669.9	6.6 g Glenium 3000 NS
TOTAL												
$\frac{g}{453.59} \times 1 / 8.33 \times 1 / sg^* = gal \quad lb = \frac{g}{1000} \times 2.20462 \quad 453.59 g = lb \quad F = C \times [1 + (E - D) / 100] \quad H = G - [A + B] - [F - C]$												

* Specific gravity.

	Admixtures				Sand				Water		Cement	Comments
ID	Amount to add		Water in admix		Net ssd (g)	Abs (%)	MC (%)	To Add Wgt (g)	Net (g)	To Add (g)	To Add (g)	
Mix/% solids	RC-CNI (g)	P20+ (g)	RC-CNI (g)	P20+ (g)								
	sg=1.295 % solid 32.5	sg=1.35 % solid 40.0	A	B	C	D	E	F	G	H	I	Glenium: sg=1.08; % sol- ids=30
9/0					8799.6	1.1	.16	8716.88	2037.3	2037.3	5991.9	w/c = 0.34
9/1	23.56	31.59	15.90	18.95	8799.6	1.1	.16	8716.88	2037.3	2085.17	5991.9	6.6 g Glenium 3000 NS
9/3	61.25	105.29	41.35	63.17	8799.6	1.1	.16	8716.88	2037.3	2015.5	5991.9	6.6 g Glenium 3000 NS
9/6	122.51	205.31	82.69	123.18	8799.6	1.1	.12	8713.4	2037.3	1917.63	5991.9	6.6 g Glenium 3000 NS
9/9	183.76	310.59	124.04	186.36	8799.6	1.1	.10	8711.6	2037.3	1814.9	5991.9	6.6 g Glenium 3000 NS
9/12	245.02	415.88	165.39	249.53	8799.6	1.1	.10	8711.6	2037.3	1710.38	5991.9	6.6 g Glenium 3000 NS
9/16	329.83	547.48	222.63	328.49	8799.6	1.1	.13	8714.2	2037.3	1571.58	5991.9	6.6 g Glenium 3000 NS
9/20	414.64	684.35	279.88	410.61	8799.6	1.1	.16	8716.88	2037.3	1429.53	5991.9	6.6 g Glenium 3000 NS
9/24	494.74	821.23	333.95	492.74	8799.6	1.1	.16	8716.88	2037.3	1293.33	5991.9	6.6 g Glenium 3000 NS
TOTAL												
$\frac{g}{453.59} \times 1 / 8.33 \times 1 / sg^* = gal \quad lb = \frac{g}{1000} \times 2.20462 \quad 453.59 g = lb \quad F = C \times [1 + (E - D) / 100] \quad H = G - [A + B] - [F - C]$												

* Specific gravity.

ID	Admixtures				Sand				Water		Cement	Comments
	Amount to add		Water in admix		Net ssd (g)	Abs (%)	MC (%)	To Add Wgt (g)	Net (g)	To Add (g)	To Add (g)	
Mix/% solids	RC-CNI (g)	P20+ (g)	RC-CNI (g)	P20+ (g)								
	sg=1.295 % solid 32.5	sg=1.35 % solid 40.0	A	B	C	D	E	F	G	H	I	Glenium: sg=1.08; % sol- ids=30
11/0.4					8291.6	1.1	.08	8207	1989.5	2074.1	6631.5	w/c = 0.30 Glen 9.32 g = 2 oz/cwt 70% H2O; 28.2g added = 6 oz/cwt
11/1.29	18.12	34.96	12.23	20.97	8291.6	1.1	.09	8207.9	1989.5	2040	6631.5	19.7 g Glenium
11/3.36	54.37	104.87	36.7	62.92	8291.6	1.1	.06	8205.4	1989.5	1976.08	6631.5	25.8 g Glenium
11/6.17	108.73	209.74	73.4	125.85	8291.6	1.1	.06	8205.4	1989.5	1876.5	6631.5	13.8 g Glenium
11/9.03	163.1	314.6	110.09	188.77	8291.6	1.1	.06	8205.4	1989.5	1776.84	6631.5	2.48 g Glenium
11/12	217.46	419.48	146.79	251.69	8291.6	1.1	.11	8209.5	1989.5	1673.12	6631.5	
11/16	285.42	565.14	192.66	339.08	8291.6	1.1	.11	8209.5	1989.5	1539.86	6631.5	
11/20	362.45	699.14	244.65	419.48	8291.6	1.1	.09	8207.9	1989.5	1409.07	6631.5	
11/24	434.94	838.97	293.59	503.38	8291.6	1.1	.1	8208.68	1989.5	1275.45	6631.5	
$g/453.59 \times 1/8.33 \times 1/sg^* = gal \quad lb = g/1000 \times 2.20462 \quad 453.59 g = lb \quad F = C \times [1 + (E - D)/100] \quad H = G - [A + B] - [F - C]$												

* Specific gravity.

APPENDIX B: Freeze-thaw data from individual mortar beams*

Table B1.

	Hz	RDME	Hz	RDME	Hz	RDME	RDME
Cycles	5/0*		5/0		5/0		Avg 5/0
0	2787	100.00	2762	100.00	2750	100.00	100.00
16	2775	99.14	2706	95.99	2743	99.49	98.21
46	2568	84.90	2493	81.47	2570	87.34	84.57
68	2468	78.42	2400	75.50	2493	82.18	78.70
92	2400	74.16	2300	69.34	2400	76.17	73.22
132	2256	65.52	2100	57.81	2337	72.22	65.18
156	2168	60.51	2000	52.43	2281	68.80	60.58
185	1975	50.22	1750	40.14	2125	59.71	50.02
	5/1		5/1		5/1		Avg 5/1
0	2781	100.00	2793	100.00	2775	100.00	100.00
16	2731	96.44	2750	96.94	2737	97.28	96.89
46	2525	82.44	2593	86.19	2600	87.79	85.47
68	2450	77.61	2506	80.50	2518	82.34	80.15
92	2425	76.04	2483	79.03	2475	79.55	78.21
132	2356	71.77	2418	74.95	2337	70.92	72.55
156	2275	66.92	2337	70.01	2281	67.57	68.17
185	2200	62.58	2200	62.04	2181	61.77	62.13
209	2118	58.00	2093	56.16	2068	55.54	56.57
	5/3		5/3		5/3		Avg 5/3
0	2825	100.00	2768	100.00	2781	100.00	100.00
16	2756	95.17	2718	96.42	2750	97.78	96.46
46	2600	84.71	2643	91.17	2681	92.94	89.60
68	2550	81.48	2585	87.21	2656	91.21	86.64
92	2525	79.89	2543	84.40	2625	89.10	84.46
132	2468	76.32	2425	76.75	2640	90.12	81.06
156	2468	76.32	2350	72.08	2631	89.50	79.30
185	2437	74.42	2275	67.55	2612	88.22	76.73
209	2412	72.90	2200	63.17	2593	86.94	74.34
253	2368	70.26	2056	55.17	2556	84.47	69.97
306	2306	66.63	1881	46.18	2506	81.20	64.67

* The averages were used to develop Figure 10 in this report. (Note: * Mix ID/admixture concentration).

	Hz	RDME	Hz	RDME	Hz	RDME	RDME
	5/6		5/6		5/6		Avg 5/6
0	2831	100.00	2812	100.00	2818	100.00	100.00
16	2737	93.47	2725	93.91	2700	91.80	93.06
46	2660	88.28	2668	90.02	2637	87.57	88.62
68	2612	85.13	2600	85.49	2600	85.13	85.25
92	2575	82.73	2568	83.40	2585	84.15	83.43
132	2450	74.89	2537	81.40	2550	81.88	79.39
156	2425	73.37	2543	81.78	2540	81.24	78.80
185	2375	70.38	2525	80.63	2500	78.70	76.57
209	2325	67.45	2512	79.80	2500	78.70	75.32
253	2268	64.18	2493	78.60	2490	78.08	73.62
306	2220	61.49	2462	76.66	2460	76.21	71.45
	5/9		5/9		5/9		Avg 5/9
0	2737	100.00	2743	100.00	2750	100.00	100.00
16	2700	97.31	2706	97.32	2700	96.40	97.01
46	2631	92.40	2637	92.42	2631	91.53	92.12
68	2600	90.24	2600	89.85	2600	89.39	89.82
92	2581	88.93	2587	88.95	2612	90.22	89.36
132	2500	83.43	2518	84.27	2562	86.79	84.83
156	2487	82.57	2512	83.87	2575	87.68	84.70
185	2470	81.44	2512	83.87	2568	87.20	84.17
209	2462	80.91	2512	83.87	2575	87.68	84.15
253	2450	80.13	2500	83.07	2568	87.20	83.47
306	2437	79.28	2481	81.81	2560	86.66	82.58
	5/12		5/12		5/12		Avg 5/12
0	2750	100.00	2731	100.00	2731	100.00	100.00
16	2743	99.49	2737	100.44	2718	99.05	99.66
46	2700	96.40	2712	98.61	2700	97.74	97.58
68	2680	94.97	2693	97.24	2681	96.37	96.19
92	2631	91.53	2631	92.81	2662	95.01	93.12
132	2560	86.66	2562	88.01	2625	92.39	89.02
156	2525	84.31	2568	88.42	2631	92.81	88.51
185	2506	83.04	2568	88.42	2637	93.23	88.23
209	2500	82.64	2581	89.32	2631	92.81	88.26
253	2506	83.04	2581	89.32	2637	93.23	88.53
306	2506	83.04	2587	89.73	2643	93.66	88.81

	Hz	RDME	Hz	RDME	Hz	RDME	RDME
	5/16		5/16		5/16		Avg 5/16
0	2681	100.00	2731	100.00	2693	100.00	100.00
16	2675	99.55	2725	99.56	2681	99.11	99.41
46	2612	94.92	2681	96.37	2637	95.88	95.73
68	2500	86.95	2560	87.87	2550	89.66	88.16
92	2412	80.94	2406	77.62	2468	83.99	80.85
132	2300	73.60	2250	67.88	2280	71.68	71.05
156	2200	67.34	2100	59.13	2110	61.39	62.62
185	1910	50.75	1925	49.68	1937	51.74	50.72
	5/20		5/20		5/20		Avg 5/20
0	2662	100.00	2643	100.00	2631	100.00	100.00
16	2631	97.68	2631	99.09	2612	98.56	98.45
46	2537	90.83	2537	92.14	2537	92.98	91.98
68	2281	73.42	2268	73.64	2281	75.16	74.07
92	1981	55.38	2000	57.26	1956	55.27	55.97
132	1468	30.41	1468	30.85	1500	32.50	31.26
	5/24		5/24		5/24		Avg 5/24
0	2593	100.00	2568	100.00	2587	100.00	100.00
16	2406	86.10	2400	87.34	2300	79.04	84.16
46	1662	41.08	1887	54.00	1787	47.72	47.60
68	706	7.41	1137	19.60	1112	18.48	15.16

Table B2.

	Hz	RDME	Hz	RDME	Hz	RDME	RDME
Cycles	6/0		6/0		6/0		Avg 6/0
0	2781	100.00	2818	100.00	2768	100.00	100.00
21	2731	96.44	2781	97.39	2731	97.34	97.06
51	2612	88.22	2631	87.17	2600	88.23	87.87
96	2456	77.99	2456	75.96	2450	78.34	77.43
133	2318	69.47	2287	65.86	2331	70.92	68.75
154	2250	65.46	2193	60.56	2256	66.43	64.15
192	2043	53.97	1968	48.77	2050	54.85	52.53
	6/1		6/1		6/1		Avg 6/1
0	2812	100.00	2812	100.00	2825	100.00	100.00
21	2762	96.48	2793	98.65	2787	97.33	97.49
51	2662	89.62	2668	90.02	2700	91.35	90.33
96	2537	81.40	2531	81.01	2593	84.25	82.22
133	2418	73.94	2381	71.69	2531	80.27	75.30

	Hz	RDME	Hz	RDME	Hz	RDME	RDME
154	2375	71.33	2318	67.95	2481	77.13	72.14
192	2281	65.80	2143	58.08	2343	68.79	64.22
229	2206	61.54	1993	50.23	2162	58.57	56.78
	6/3		6/3		6/3		Avg 6/3
0	2800	100.00	2812	100.00	2825	100.00	100.00
21	2750	96.46	2775	97.39	2768	96.01	96.62
51	2662	90.39	2706	92.60	2681	90.07	91.02
96	2581	84.97	2637	87.94	2581	83.47	85.46
133	2493	79.27	2556	82.62	2525	79.89	80.59
154	2475	78.13	2531	81.01	2487	77.50	78.88
192	2400	73.47	2450	75.91	2393	71.75	73.71
229	2318	68.53	2400	72.84	2300	66.29	69.22
258	2231	63.49	2400	72.84	2193	60.26	65.53
301	2250	64.57	2400	72.84	2168	58.90	65.44
	6/6		6/6		6/6		Avg 6/6
0	2806	100.00	2878	100.00	2800	100.00	100.00
21	2718	93.83	2681	86.78	2718	94.23	91.61
51	2637	88.32	2606	81.99	2656	89.98	86.76
96	2512	80.14	2468	73.54	2562	83.72	79.13
133	2387	72.37	2325	65.26	2456	76.94	71.52
154	2343	69.72	2250	61.12	2400	73.47	68.10
192	2225	62.88	2143	55.45	2331	69.31	62.54
229	2162	59.37	1968	46.76	2293	67.06	57.73
	6/9		6/9		6/9		Avg 6/9
0	2700	100.00	2700	100.00	2725	100.00	100.00
21	2606	93.16	2612	93.59	2650	94.57	93.77
51	2575	90.96	2568	90.46	2618	92.30	91.24
96	2531	87.87	2506	86.15	2600	91.04	88.35
133	2481	84.44	2387	78.16	2550	87.57	83.39
154	2475	84.03	2368	76.92	2531	86.27	82.41
192	2456	82.74	2287	71.75	2506	84.57	79.69
229	2450	82.34	2275	71.00	2493	83.70	79.01
258	2450	82.34	2243	69.01	2493	83.70	78.35
301	2493	85.25	2300	72.57	2518	85.38	81.07
	6/12		6/12		6/12		Avg 6/12
0	2693	100.00	2662	100.00	2681	100.00	100.00
21	2600	93.21	2562	92.63	2587	93.11	92.98
51	2568	90.93	2518	89.47	2562	91.32	90.58
96	2512	87.01	2418	82.51	2506	87.37	85.63
133	2437	81.89	2268	72.59	2381	78.87	77.78

	Hz	RDME	Hz	RDME	Hz	RDME	RDME
154	2381	78.17	2218	69.42	2350	76.83	74.81
192	2350	76.15	2125	63.72	2287	72.77	70.88
229	2312	73.71	2100	62.23	2287	72.77	69.57
258	2293	72.50	2087	61.47	2281	72.39	68.78
301	2300	72.94	2100	62.23	2300	73.60	69.59
	6/16		6/16		6/16		Avg 6/16
0	2618	100.00	2606	100.00	2625	100.00	100.00
21	2406	84.46	2381	83.48	2462	87.97	85.30
51	1981	57.26	1937	55.25	2231	72.23	61.58
96	962	13.50	918	12.41	1500	32.65	19.52
	6/20		6/20		6/20		Avg 6/20
0	2587	100.00	2581	100.00	2568	100.00	100.00
21	2037	62.00	2137	68.55	2006	61.02	63.86
51	1006	15.12	1300	25.37	843	10.78	17.09
	6/24		6/24		6/24		Avg 6/24
0	2500	100.00	2531	100.00	2500	100.00	100.00
21	1025	16.81	1312	26.87	1143	20.90	21.53

Table B3.

	Hz	RDME	Hz	RDME	Hz	RDME	RDME
Cycles	8/0		8/0		8/0		Avg 8/0
0	2837	100.00	2843	100.00	2843	100.00	100.00
21	2768	95.19	2831	99.16	2812	97.83	97.39
51	2737	93.07	2781	95.69	2768	94.79	94.52
96	2737	93.07	2781	95.69	2756	93.97	94.24
133	2718	91.79	2781	95.69	2756	93.97	93.82
154	2725	92.26	2781	95.69	2750	93.56	93.84
192	2712	91.38	2781	95.69	2743	93.09	93.39
229	2700	90.58	2793	96.51	2750	93.56	93.55
258	2687	89.71	2793	96.51	2743	93.09	93.10
301	2693	90.11	2800	97.00	2750	93.56	93.56
	8/1		8/1		8/1		Avg 8/1
0	2825	100.00	2837	100.00	2856	100.00	100.00
21	2775	96.49	2831	99.58	2850	99.58	98.55
51	2743	94.28	2781	96.09	2787	95.23	95.20
96	2750	94.76	2781	96.09	2781	94.82	95.22
133	2743	94.28	2775	95.68	2787	95.23	95.06
154	2756	95.17	2775	95.68	2787	95.23	95.36
192	2756	95.17	2775	95.68	2787	95.23	95.36

	Hz	RDME	Hz	RDME	Hz	RDME	RDME
229	2768	96.01	2787	96.51	2787	95.23	95.91
258	2768	96.01	2781	96.09	2787	95.23	95.77
301	2775	96.49	2793	96.92	2800	96.12	96.51
	8/3		8/3		8/3		Avg 8/3
0	2875	100.00	2875	100.00	2887	100.00	100.00
21	2881	100.42	2868	99.51	2887	100.00	99.98
51	2812	95.67	2768	92.70	2825	95.75	94.70
96	2806	95.26	2756	91.89	2812	94.87	94.01
133	2806	95.26	2750	91.49	2812	94.87	93.87
154	2812	95.67	2750	91.49	2812	94.87	94.01
192	2818	96.07	2725	89.84	2806	94.47	93.46
229	2818	96.07	2662	85.73	2787	93.19	91.67
258	2818	96.07	2612	82.54	2768	91.93	90.18
301	2825	96.55	2593	81.34	2756	91.13	89.68
	8/6		8/6		8/6		Avg 8/6
0	2906	100.00	2912	100.00	2918	100.00	100.00
21	2868	97.40	2881	97.88	2912	99.59	98.29
51	2800	92.84	2837	94.92	2862	96.20	94.65
96	2800	92.84	2831	94.51	2850	95.39	94.25
133	2800	92.84	2836	94.85	2856	95.80	94.49
154	2812	93.64	2843	95.32	2862	96.20	95.05
192	2812	93.64	2856	96.19	2868	96.60	95.48
229	2806	93.24	2862	96.60	2875	97.07	95.64
258	2781	91.58	2868	97.00	2875	97.07	95.22
301	2800	92.84	2881	97.88	2887	97.89	96.20
	8/9		8/9		8/9		Avg 8/9
0	2912	100.00	2887	100.00	2887	100.00	100.00
21	2850	95.79	2818	95.28	2831	96.16	95.74
51	2806	92.85	2787	93.19	2793	93.59	93.21
96	2800	92.46	2806	94.47	2793	93.59	93.51
133	2800	92.46	2825	95.75	2825	95.75	94.65
154	2812	93.25	2837	96.57	2831	96.16	95.32
192	2812	93.25	2856	97.86	2850	97.45	96.19
229	2818	93.65	2862	98.28	2856	97.86	96.60
258	2831	94.51	2862	98.28	2862	98.28	97.02
301	2843	95.32	2881	99.58	2881	99.58	98.16
	8/12		8/12		8/12		Avg 8/12
0	2912	100.00	2931	100.00	2906	100.00	100.00
21	2862	96.60	2900	97.90	2856	96.59	97.03
51	2800	92.46	2850	94.55	2812	93.64	93.55

	Hz	RDME	Hz	RDME	Hz	RDME	RDME
96	2818	93.65	2868	95.75	2831	94.90	94.77
133	2837	94.92	2868	95.75	2850	96.18	95.62
154	2856	96.19	2875	96.22	2856	96.59	96.33
192	2862	96.60	2881	96.62	2875	97.88	97.03
229	2875	97.47	2887	97.02	2875	97.88	97.46
258	2875	97.47	2893	97.42	2881	98.29	97.73
301	2893	98.70	2900	97.90	2893	99.11	98.57
	8/16		8/16		8/16		Avg 8/16
0	2893	100.00	2893	100.00	2881	100.00	100.00
21	2862	97.87	2862	97.87	2831	96.56	97.43
51	2812	94.48	2818	94.88	2787	93.58	94.31
96	2800	93.67	2806	94.08	2787	93.58	93.78
133	2806	94.08	2812	94.48	2787	93.58	94.05
154	2818	94.88	2818	94.88	2793	93.98	94.58
192	2825	95.35	2818	94.88	2806	94.86	95.03
229	2837	96.17	2825	95.35	2812	95.27	95.60
258	2837	96.17	2825	95.35	2825	96.15	95.89
301	2856	97.46	2843	96.57	2837	96.97	97.00
	8/20		8/20		8/20		Avg 8/20
0	2881	100.00	2887	100.00	2906	100.00	100.00
21	2806	94.86	2806	94.47	2818	94.04	94.45
51	2725	89.46	2718	88.64	2750	89.55	89.22
96	2718	89.00	2668	85.40	2750	89.55	87.99
133	2706	88.22	2675	85.85	2712	87.09	87.06
154	2706	88.22	2668	85.40	2675	84.73	86.12
192	2706	88.22	2618	82.23	2625	81.60	84.02
229	2687	86.99	2568	79.12	2581	78.88	81.66
258	2687	86.99	2543	77.59	2568	78.09	80.89
301	2718	89.00	2550	78.02	2575	78.52	81.85
	8/24		8/24		8/24		Avg 8/24
0	2837	100.00	2850	100.00	2837	100.00	100.00
21	2525	79.21	2687	88.89	2656	87.65	85.25
51	2206	60.46	2462	74.63	2418	72.64	69.24
96	1800	40.26	2193	59.21	2093	54.43	51.30
133	1450	26.12	1856	42.41	1868	43.35	37.30

Table B4.

	Hz	RDME	Hz	RDME	Hz	RDME	RDME
Cycles	9/0		9/0		9/0		Avg 9/0
0	2856	100.00	2837	100.00	2850	100.00	100.00
21	2793	95.64	2787	96.51	2781	95.22	95.79
58	2793	95.64	2800	97.41	2781	95.22	96.09
102	2787	95.23	2800	97.41	2787	95.63	96.09
153	2793	95.64	2800	97.41	2793	96.04	96.36
183	2793	95.64	2800	97.41	2800	96.52	96.52
237	2781	94.82	2800	97.41	2800	96.52	96.25
266	2787	95.23	2812	98.25	2806	96.94	96.80
310	2793	95.64	2812	98.25	2806	96.94	96.94
	9/1		9/1		9/1		Avg 9/1
0	2881	100.00	2850	100.00	2850	100.00	100.00
21	2880	99.93	2787	95.63	2787	95.63	97.06
58	2806	94.86	2793	96.04	2793	96.04	95.65
102	2812	95.27	2800	96.52	2793	96.04	95.94
153	2812	95.27	2812	97.35	2812	97.35	96.66
183	2818	95.67	2818	97.77	2818	97.77	97.07
237	2825	96.15	2825	98.25	2831	98.67	97.69
266	2831	96.56	2825	98.25	2837	99.09	97.97
310	2837	96.97	2818	97.77	2843	99.51	98.08
	9/3		9/3		9/3		Avg 9/3
0	2912	100.00	2887	100.00	2906	100.00	100.00
21	2825	94.11	2781	92.79	2812	93.64	93.51
58	2825	94.11	2775	92.39	2812	93.64	93.38
102	2825	94.11	2775	92.39	2825	94.50	93.67
153	2831	94.51	2787	93.19	2837	95.31	94.34
183	2837	94.92	2793	93.59	2837	95.31	94.61
237	2843	95.32	2800	94.06	2850	96.18	95.19
266	2856	96.19	2800	94.06	2862	96.99	95.75
310	2862	96.60	2793	93.59	2868	97.40	95.86
	9/6		9/6		9/6		Avg 9/6
0	2943	100.00	2931	100.00	2893	100.00	100.00
21	2831	92.53	2818	92.44	2793	93.21	92.73
58	2825	92.14	2812	92.04	2793	93.21	92.46
102	2837	92.93	2825	92.90	2806	94.08	93.30
153	2850	93.78	2837	93.69	2818	94.88	94.12
183	2856	94.18	2850	94.55	2818	94.88	94.54

	Hz	RDME	Hz	RDME	Hz	RDME	RDME
237	2862	94.57	2856	94.95	2837	96.17	95.23
266	2875	95.43	2868	95.75	2843	96.57	95.92
310	2881	95.83	2868	95.75	2850	97.05	96.21
	9/9		9/9		9/9		Avg 9/9
0	2956	100.00	2950	100.00	2950	100.00	100.00
21	2856	93.35	2856	93.73	2862	94.12	93.73
58	2856	93.35	2856	93.73	2856	93.73	93.60
102	2856	93.35	2862	94.12	2856	93.73	93.73
153	2875	94.59	2875	94.98	2881	95.38	94.98
183	2881	94.99	2881	95.38	2887	95.77	95.38
237	2900	96.25	2893	96.17	2900	96.64	96.35
266	2912	97.05	2900	96.64	2912	97.44	97.04
310	2918	97.45	2900	96.64	2918	97.84	97.31
	9/12		9/12		9/12		Avg 9/12
0	2937	100.00	2931	100.00	2950	100.00	100.00
21	2843	93.70	2831	93.29	2862	94.12	93.71
58	2831	92.91	2837	93.69	2862	94.12	93.57
102	2831	92.91	2843	94.09	2868	94.52	93.84
153	2843	93.70	2850	94.55	2875	94.98	94.41
183	2856	94.56	2862	95.35	2881	95.38	95.09
237	2868	95.36	2868	95.75	2887	95.77	95.63
266	2881	96.22	2875	96.22	2893	96.17	96.20
310	2893	97.03	2875	96.22	2900	96.64	96.63
	9/16		9/16		9/16		Avg 9/16
0	2937	100.00	2912	100.00	2931	100.00	100.00
21	2862	94.96	2793	91.99	2843	94.09	93.68
58	2862	94.96	2793	91.99	2837	93.69	93.55
102	2862	94.96	2800	92.46	2843	94.09	93.83
153	2862	94.96	2806	92.85	2850	94.55	94.12
183	2868	95.36	2812	93.25	2856	94.95	94.52
237	2875	95.82	2825	94.11	2862	95.35	95.09
266	2881	96.22	2831	94.51	2868	95.75	95.49
310	2887	96.62	2843	95.32	2875	96.22	96.05
	9/20		9/20		9/20		Avg 9/20
0	2900	100.00	2881	100.00	2931	100.00	100.00
21	2693	86.23	2662	85.37	2718	85.99	85.87
58	2668	84.64	2581	80.26	2700	84.86	83.25
102	2637	82.68	2481	74.16	2668	82.86	79.90
153	2600	80.38	2412	70.09	2600	78.69	76.39
183	2568	78.41	2362	67.22	2568	76.76	74.13

	Hz	RDME	Hz	RDME	Hz	RDME	RDME
237	2475	72.84	2312	64.40	2456	70.21	69.15
266	2443	70.97	2306	64.07	2475	71.30	68.78
310	2406	68.83	2312	64.40	2475	71.30	68.18
	9/24		9/24		9/24		Avg 9/24
0	2731	100.00	2837	100.00	2881	100.00	100.00
21	2381	76.01	2443	74.15	2468	73.38	74.52
58	2231	66.74	2212	60.79	2256	61.32	62.95
102	1931	49.99	1906	45.14	2050	50.63	48.59

Table B5.

	Hz	RDME	Hz	RDME	Hz	RDME	RDME
Cycles	11/0		11/0		11/0		Avg 11/0
0	2931	100.00	2937	100.00	2937	100.00	100.00
16	2850	94.55	2856	94.56	2875	95.82	94.98
46	2881	96.62	2875	95.82	2881	96.22	96.22
68	2881	96.62	2881	96.22	2887	96.62	96.49
92	2862	95.35	2887	96.62	2887	96.62	96.20
132	2893	97.42	2887	96.62	2868	95.36	96.47
156	2887	97.02	2887	96.62	2893	97.03	96.89
185	2931	100.00	2893	97.03	2875	95.82	97.62
209	2900	97.90	2893	97.03	2906	97.90	97.61
253	2943	100.82	2900	97.50	2881	96.22	98.18
306	2912	98.71	2906	97.90	2912	98.30	98.30
	11/1		11/1		11/1		Avg 11/1
0	2937	100.00	2937	100.00	2943	100.00	100.00
16	2856	94.56	2887	96.62	2881	95.83	95.67
46	2887	96.62	2881	96.22	2862	94.57	95.81
68	2887	96.62	2856	94.56	2893	96.63	95.94
92	2887	96.62	2881	96.22	2893	96.63	96.49
132	2887	96.62	2887	96.62	2900	97.10	96.78
156	2887	96.62	2883	96.36	2900	97.10	96.69
185	2893	97.03	2900	97.50	2912	97.90	97.48
209	2900	97.50	2893	97.03	2912	97.90	97.48
253	2906	97.90	2906	97.90	2906	97.50	97.77
306	2912	98.30	2912	98.30	2918	98.31	98.31
	11/3		11/3		11/3		Avg 11/3
0	2931	100.00	2956	100.00	2956	100.00	100.00
16	2900	97.90	2868	94.13	2850	92.96	95.00
46	2875	96.22	2856	93.35	2875	94.59	94.72

	Hz	RDME	Hz	RDME	Hz	RDME	RDME
68	2856	94.95	2881	94.99	2881	94.99	94.98
92	2906	98.30	2900	96.25	2906	96.65	97.06
132	2868	95.75	2912	97.05	2906	96.65	96.48
156	2906	98.30	2912	97.05	2912	97.05	97.46
185	2912	98.71	2918	97.45	2918	97.45	97.87
209	2912	98.71	2918	97.45	2925	97.91	98.02
253	2918	99.11	2925	97.91	2931	98.32	98.45
306	2925	99.59	2931	98.32	2931	98.32	98.74
	11/6		11/6		11/6		Avg 11/6
0	2981	100.00	2956	100.00	2968	100.00	100.00
16	2912	95.42	2856	93.35	2862	92.98	93.92
46	2868	92.56	2918	97.45	2868	93.37	94.46
68	2862	92.18	2925	97.91	2868	93.37	94.49
92	2900	94.64	2912	97.05	2906	95.87	95.85
132	2912	95.42	2912	97.05	2906	95.87	96.11
156	2918	95.82	2906	96.65	2912	96.26	96.24
185	2925	96.28	2912	97.05	2918	96.66	96.66
209	2925	96.28	2918	97.45	2925	97.12	96.95
253	2931	96.67	2925	97.91	2931	97.52	97.37
306	2943	97.47	2931	98.32	2943	98.32	98.03
	11/9		11/9		11/9		Avg 11/9
0	3025	100.00	3006	100.00	3006	100.00	100.00
16	2887	91.08	2918	94.23	2887	92.24	92.52
46	2887	91.08	2925	94.68	2893	92.62	92.80
68	2893	91.46	2950	96.31	2918	94.23	94.00
92	2912	92.67	2937	95.46	2937	95.46	94.53
132	2918	93.05	2937	95.46	2943	95.85	94.79
156	2918	93.05	2943	95.85	2943	95.85	94.92
185	2918	93.05	2956	96.70	2950	96.31	95.35
209	2937	94.27	2950	96.31	2956	96.70	95.76
253	2937	94.27	2968	97.49	2962	97.09	96.28
306	2943	94.65	2975	97.95	2962	97.09	96.56
	11/12		11/12		11/12		Avg 11/12
0	3050	100.00	3050	100.00	3025	100.00	100.00
16	2956	93.93	2943	93.11	2956	95.49	94.18
46	2956	93.93	2993	96.30	2950	95.10	95.11
68	2956	93.93	2968	94.70	2956	95.49	94.71
92	2950	93.55	2968	94.70	2968	96.27	94.84
132	2950	93.55	2968	94.70	2975	96.72	94.99
156	2950	93.55	2968	94.70	2975	96.72	94.99

	Hz	RDME	Hz	RDME	Hz	RDME	RDME
185	2956	93.93	2981	95.53	2981	97.11	95.52
209	2962	94.31	2981	95.53	2981	97.11	95.65
253	2968	94.70	3000	96.75	2987	97.50	96.32
306	2975	95.14	3000	96.75	2993	97.90	96.60
	11/16		11/16		11/16		Avg 11/16
0	3037	100.00	3043	100.00	3025	100.00	100.00
16	2912	91.94	2943	93.54	2943	94.65	93.38
46	2893	90.74	2950	93.98	2943	94.65	93.12
68	2893	90.74	2937	93.15	2950	95.10	93.00
92	2925	92.76	2925	92.39	2931	93.88	93.01
132	2925	92.76	2918	91.95	2931	93.88	92.87
156	2925	92.76	2918	91.95	2931	93.88	92.87
185	2931	93.14	2925	92.39	2937	94.27	93.27
209	2925	92.76	2925	92.39	2937	94.27	93.14
253	2943	93.91	2937	93.15	2943	94.65	93.90
306	2950	94.35	2943	93.54	2950	95.10	94.33
	11/20		11/20		11/20		Avg 11/20
0	3018	100.00	3031	100.00	3031	100.00	100.00
16	2825	87.62	2831	87.24	2800	85.34	86.73
46	2793	85.65	2831	87.24	2843	87.98	86.95
68	2800	86.08	2831	87.24	2843	87.98	87.10
92	2850	89.18	2881	90.35	2850	88.41	89.31
132	2881	91.13	2881	90.35	2856	88.79	90.09
156	2881	91.13	2868	89.53	2831	87.24	89.30
185	2881	91.13	2900	91.54	2831	87.24	89.97
209	2875	90.75	2900	91.54	2887	90.72	91.00
253	2875	90.75	2906	91.92	2831	87.24	89.97
306	2868	90.31	2900	91.54	2831	87.24	89.70
	11/24		11/24		11/24		Avg 11/24
0	2950	100.00	2981	100.00	2962	100.00	100.00
16	2631	79.54	2593	75.66	2587	76.28	77.16
46	2506	72.16	2575	74.62	2543	73.71	73.50
68	2481	70.73	2550	73.17	2462	69.09	71.00
92	2450	68.97	2512	71.01	2450	68.42	69.47
132	2431	67.91	2356	62.46	2400	65.65	65.34
156	2362	64.11	2306	59.84	2237	57.04	60.33
185	2293	60.42	2112	50.20	2150	52.69	54.43

APPENDIX C: Relationship between length-change and temperature for antifreeze mortar beams

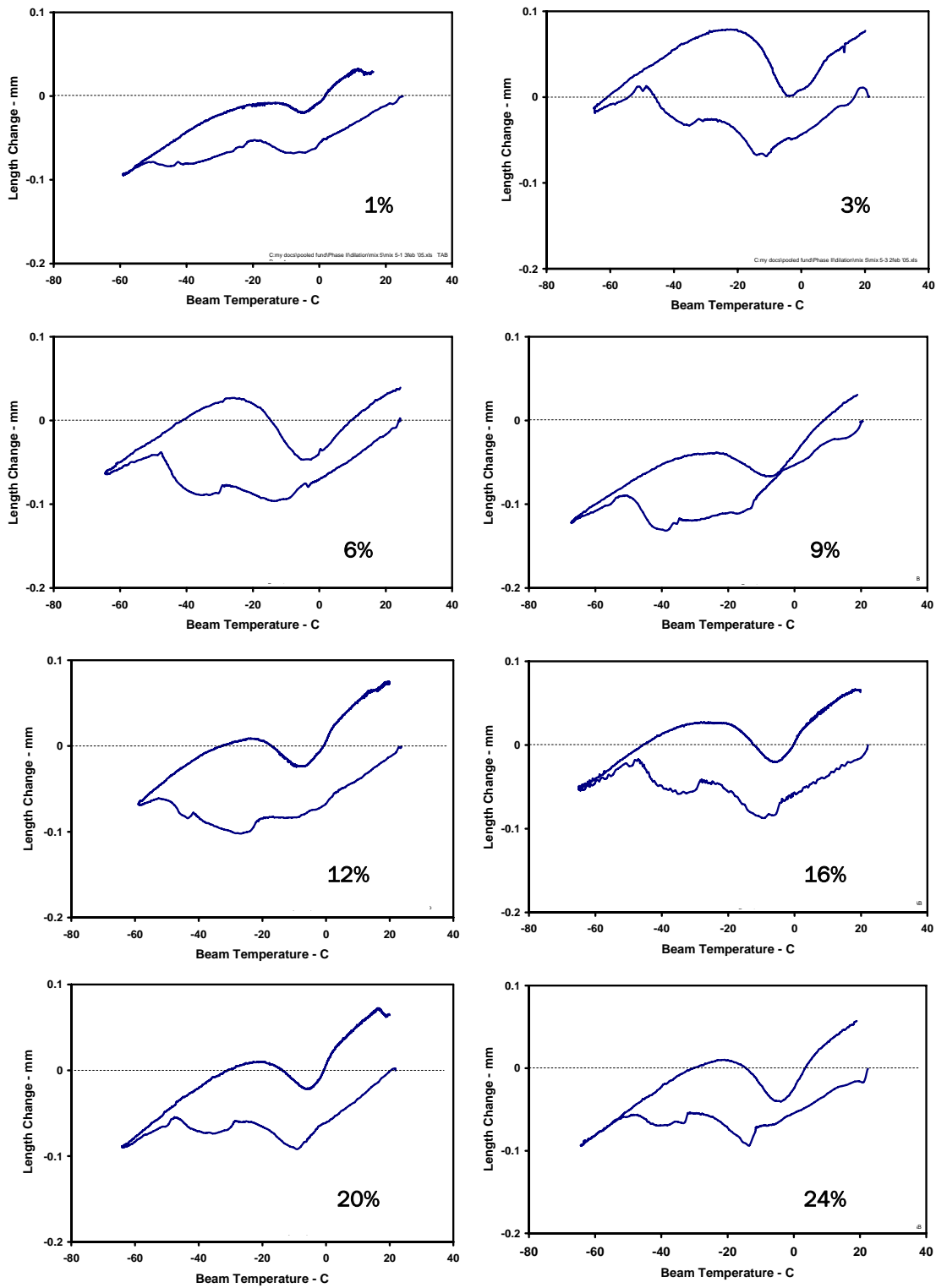


Figure C1. Mix 5 (% = [wgt of solids in the admixture/total wgt water in the mortar] x 100)

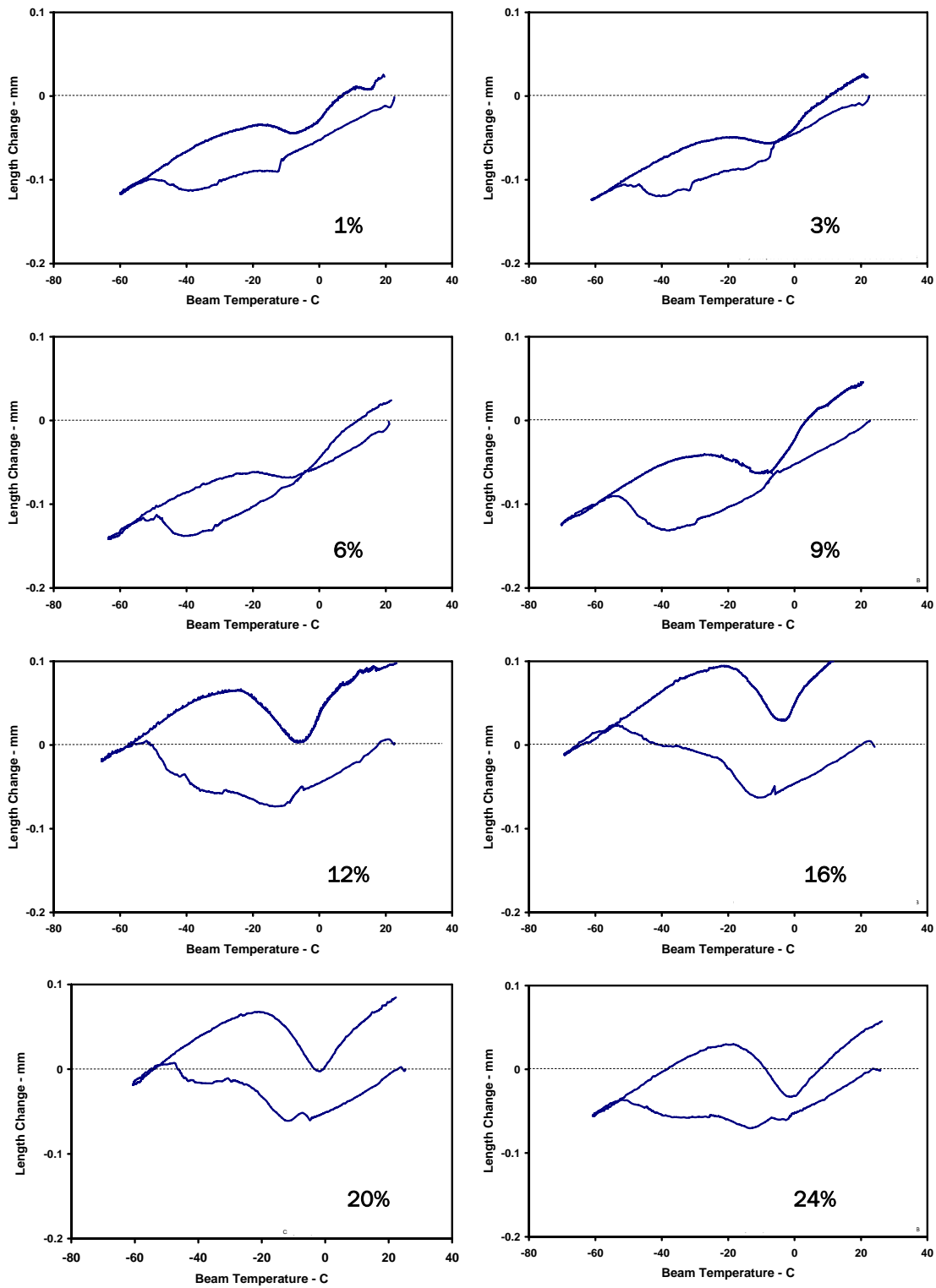


Figure C2. Mix 6 (% = [wgt of solids in the admixture/total wgt water in the mortar] x 100).

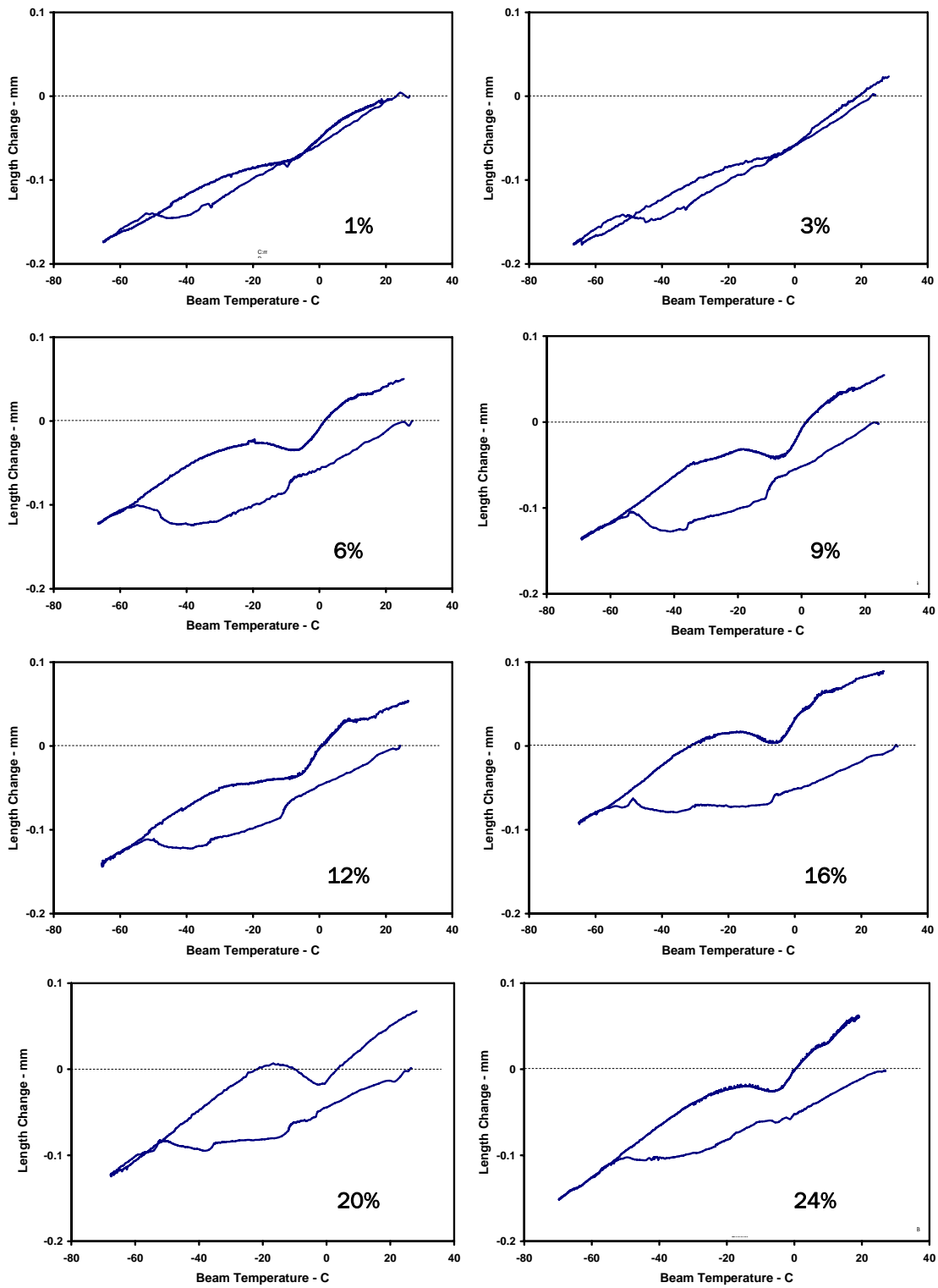


Figure C3. Mix 8 (% = [wgt of solids in the admixture/total wgt water in the mortar] x 100).

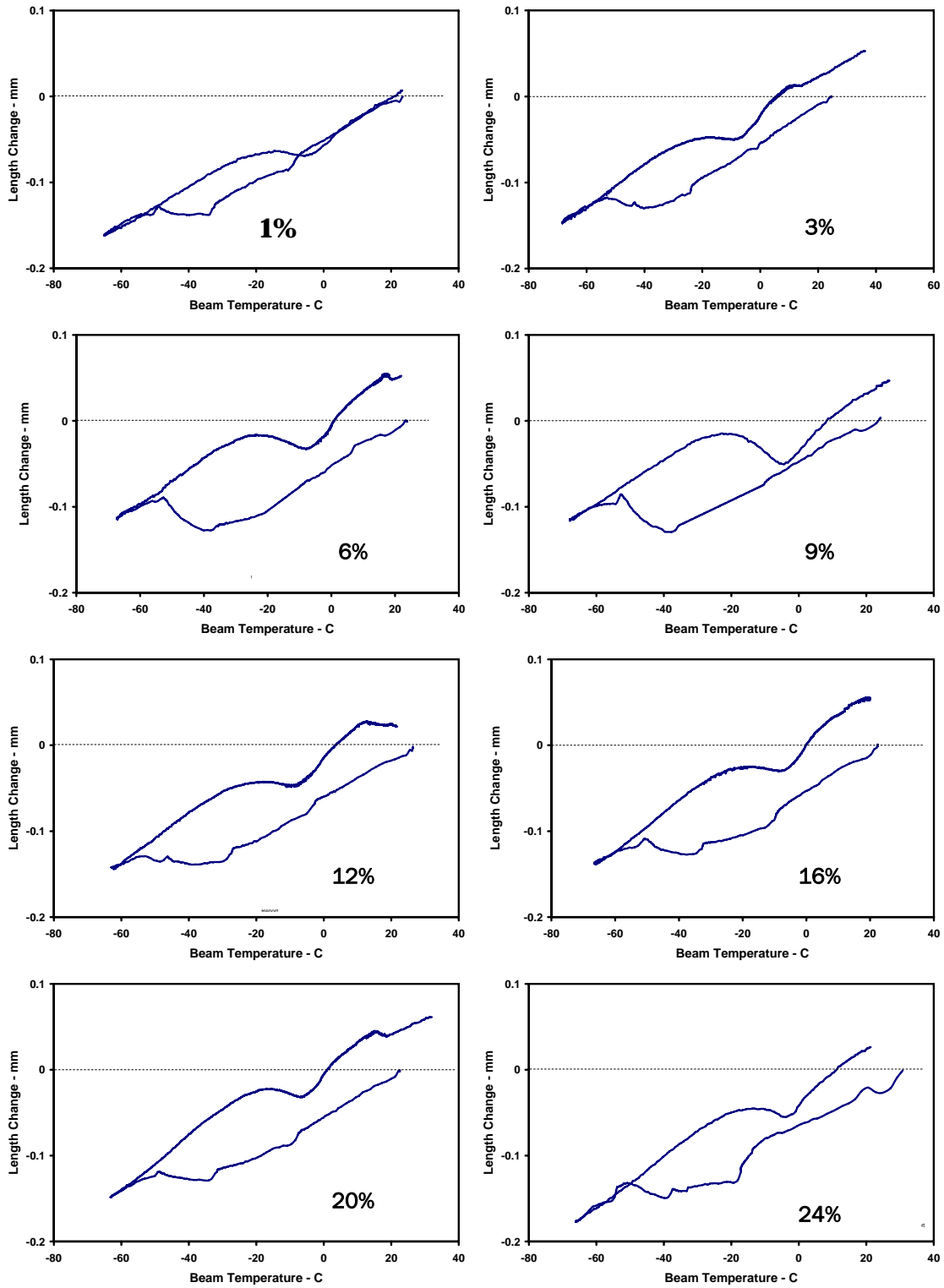


Figure C4. Mix 9 (% = [wgt of solids in the admixture/total wgt water in the mortar] x 100).

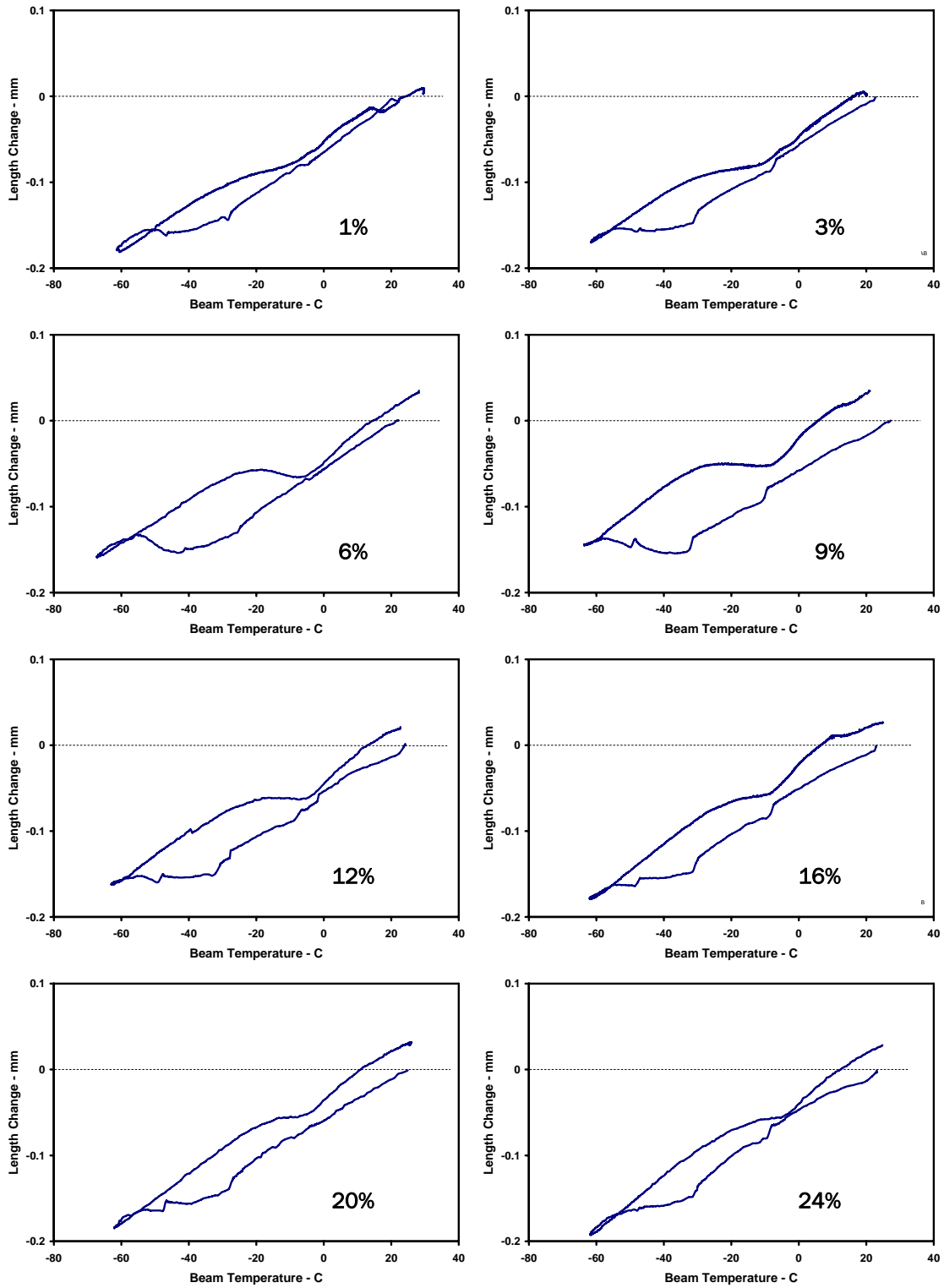


Figure C5. Mix 11 (% = [wgt of solids in the admixture/total wgt water in the mortar] x 100).

REPORT DOCUMENTATION PAGE

Form Approved
OMB No. 0704-0188

Public reporting burden for this collection of information is estimated to average 1 hour per response, including the time for reviewing instructions, searching existing data sources, gathering and maintaining the data needed, and completing and reviewing this collection of information. Send comments regarding this burden estimate or any other aspect of this collection of information, including suggestions for reducing this burden to Department of Defense, Washington Headquarters Services, Directorate for Information Operations and Reports (0704-0188), 1215 Jefferson Davis Highway, Suite 1204, Arlington, VA 22202-4302. Respondents should be aware that notwithstanding any other provision of law, no person shall be subject to any penalty for failing to comply with a collection of information if it does not display a currently valid OMB control number. **PLEASE DO NOT RETURN YOUR FORM TO THE ABOVE ADDRESS.**

1. REPORT DATE (DD-MM-YYYY) April 2006		2. REPORT TYPE		3. DATES COVERED (From - To)	
4. TITLE AND SUBTITLE Extending the Season for Concrete Construction and Repair Phase II—Defining Engineering Parameters				5a. CONTRACT NUMBER	
				5b. GRANT NUMBER	
				5c. PROGRAM ELEMENT NUMBER	
6. AUTHOR(S) Charles J. Korhonen				5d. PROJECT NUMBER TPF-5(075)	
				5e. TASK NUMBER	
				5f. WORK UNIT NUMBER	
7. PERFORMING ORGANIZATION NAME(S) AND ADDRESS(ES) U.S. Army Engineer Research and Development Center Cold Regions Research and Engineering Laboratory 72 Lyme Road Hanover, NH 03766				8. PERFORMING ORGANIZATION REPORT NUMBER ERDC/CRREL TR-06-08	
9. SPONSORING / MONITORING AGENCY NAME(S) AND ADDRESS(ES) U.S. Federal Highway Administration Washington, DC				10. SPONSOR/MONITOR'S ACRONYM(S)	
				11. SPONSOR/MONITOR'S REPORT NUMBER(S)	
12. DISTRIBUTION / AVAILABILITY STATEMENT Approved for public release; distribution is unlimited.					
13. SUPPLEMENTARY NOTES					
14. ABSTRACT The Phase I study, conducted prior to the work reported herein, developed the tools to design, mix, place, and cure concrete in cold weather made with various combinations of commercial admixtures. The admixtures helped to protect concrete and maintain productivity, even when the temperature of concrete falls to -5°C soon after mixing. Phase II addressed the effect of high doses of the chemical admixtures studied in Phase I. The primary finding from Phase I that led to this study was that admixtures, when used in moderate dosages, seemed improve the freeze-thaw durability of concrete. Phase II found what appears to be a maximum dosage after which freeze-thaw durability becomes a concern. That is because cement hydration can only create a finite amount of space to absorb these chemicals. Thus, for freeze protection, admixture dosages should be designed according to water content as specified in Phase I, while, for freeze-thaw durability, admixture dosages should be dictated by cement content. When using both considerations, the freeze-protection limit for enhanced freeze-thaw durable concrete can be lower than the -5°C limit set in Phase I.					
15. SUBJECT TERMS Antifreeze Cold weather concrete			Freezing point Freeze-thaw durability		
16. SECURITY CLASSIFICATION OF:			17. LIMITATION OF ABSTRACT	18. NUMBER OF PAGES	19a. NAME OF RESPONSIBLE PERSON
a. REPORT unclassified	b. ABSTRACT unclassified	c. THIS PAGE unclassified			75